TABLE 2. Methods for pretreatment and incubation with antibodies

Procedures	Combinations of antibodies			
	PSA Ki67 BrdU	β-catenin Ki67 PSA	β-catenin N-cadherin PSA	GFP KI67 PSA
primary antibodies 1* 1–3 overnight, 4°C	mouse IgG anti-Ki67	mouse IgG anti-Ki67 rabbit IgG anti-β-catenin	rabbit IgG anti-β-catenin mouse IgG anti-N-cadherin	mouse IgG anti-Ki67
↓				
Pretreatment 1*	100% Methanol	100% Methanol	100% Methanol	100% Methanol
↓				
primary antibodies 2* 1–3 overnight, 4°C	mouse IgM anti-PSA	mouse IgM anti-PSA	mouse IgM anti-PSA	mouse IgM anti-PSA rabbit IgG anti-GFP
↓				
secondary antibodies 1 + 2* 1–2 hrs, r.t.***	anti-mouse IgG + cy3** anti-mouse IgM + Cy2	anti-mouse IgG + Cy3** anti-mouse IgM + Cy5 anti-rabbit IgG + FITC	anti-mouse IgG + Cy3** anti-mouse IgM + Cy5 anti-rabbit IgG + FITC	anti-mouse IgG + Cy3** anti-mouse IgM + Cy5 anti-rabbit IgG + FITC
↓				
Pretreatment 2* 30 min, r.t.***	2N HCl			
↓				
primary antibodies 3* 1–2 overnigt, 4°C	rat IgG anti-BrdU			
↓				
secondary antibodies 3* 1–2 hrs, r.t.**	anti-rat IgG + Cy5			

The Immunohistochemical methods without pretreatments are discribed in the Materials and Methods.
*Each step was followed by washing with PBS or PBS-T. 10 min × 3 In case of incubation with HCl, Borate buffer was used for the first washing.
**anti-mouse IgG [γ]
***r.t.; at room temperature

Immunohistochemistry

The primary and secondary antibodies were diluted with PBS or 0.1% Triton X-100 in PBS (PBS-T) containing 0.1% BSA. In triple staining without pretreatment (GFAP/Ki67/Hu, S100β/Ki67/Hu, MASH-1/Ki67/Hu, GFAP/MASH-1/Hu, GFP/Hu/ki67, GFP/Hu/GFAP), free-floating vibratome sections were incubated with a mixture of primary antibodies at 4°C for 1–3 nights and then with a mixture of secondary antibodies at room temperature for 1–2 hours. Each step was followed by washing with PBS or PBS-T.

For immunostaining using anti-PSA the vibratome sections were pretreated with 100% methanol for 30 minutes to enhance the penetration of IgM antibody into neural tissues. In the case of immunostaining using anti-PSA and anti-Ki67, the sections were first incubated with mouse IgG monoclonal anti-Ki67 and then pretreated with 100% methanol for 30 minutes, because the methanol pretreatment caused artifacts in Ki67 immunostaining. For BrdU immunostaining the sections were pretreated with 2N-HCl at 37°C for 30 minutes to denature the DNA and then neutralized with Borate buffer (pH 8.5) at room temperature for 10 minutes. The sections were incubated with a primary antibody or a mixture of primary antibodies for 12–72 hours at 4°C and then with a secondary antibody or a mixture of secondary antibodies for 1–2 hours at room temperature. The detailed pretreatment and incubation with antibodies for each staining are shown in Table 2.

Finally, the sections were mounted on glass slides with a solution of 30% ethylene glycol and 25% glycerin in 0.1 M PB. The sections were examined with a Zeiss confocal laser scanning microscope 510 or 510 META with 20×, 40×, 64× objectives and, in some cases, fluorescence images were digitally zoomed 1.2× to 2×. Stacks of optical sections (0.9 and 1.8 μm in thickness) were obtained at 0.45- and 0.9-μm increments on the z-axis, respectively. The images were corrected for brightness and contrast and composed using the Zeiss LSM Image Browser and Adobe Photoshop 5.5 (San Jose, CA).

Slice culture preparation

Postnatal day 5 (P5) rats were injected stereotactically with 0.5 μL of our modified retrovirus vector, GCDNsap-EGFP retrovirus (posterior, 1.2 mm from bregma; lateral, 2.1 mm; ventral, 2 mm), as described previously (Suzuki et al., 2002; Namba et al., 2005). Three days after the retroviral injection (P8) the rats were deeply anesthetized with diethyl ether. Hippocampal slices at a thickness of 350 μm were prepared by the standard method (Stoppini et al., 1991; Sakaguchi et al., 1997). The hippocampal slices were transferred onto a collagen-coated glass bottom dish (35 mm in diameter, WillCo Wells, The Netherlands). Ninety μL of a mixture of 50% MEM (Invitrogen), 25% heat inactivated horse serum (Invitrogen), and 25% Hank's balanced salt solution (Invitrogen) supplemented with penicillin-streptomycin-glutamine (Invitrogen) and glucose at a final concentration of 6.5 mg/mL was added to the well of the glass-bottom dish (22 mm well diameter).

Time-lapse confocal imaging

Time-lapse recording was performed manually using an inverted confocal laser-scanning microscope (LSM510 META; Zeiss, Germany) and minimal laser excitation (typically 1% of an Argon 488 laser) to prevent photodamage and photobleaching. To follow the movements of the labeled cells, stacks of images were collected in the z-plane every 2 hours using a 20× objective. Between the time-points the slices were kept in a water-jacketed incubator at 37°C and 5% CO_2. Time-lapse sequences were arranged using Photoshop (Adobe Systems).

Cell counting and statistical analysis

To calculate the proportions of cell phenotypes of BrdU, Ki67 and GFP-labeled cells, confocal z-stack images were analyzed. We used 3–7 animals per group and counted 5–12 sections per animal. The chi-square test was used for statistical analysis.

The Journal of Comparative Neurology. DOI 10.1002/cne

RESULTS

BrdU experiments

In the initial experiments we examined 2-month-old rats, which are generally used in experiments on adult neurogenesis. As described previously (Seki, 2002), the SGZ of the young adult rats contained many PSA+ cells. Radially or tangentially oriented processes extended from the PSA+ cells and formed a continuous plexus consisting of their cell bodies and tangential processes along the border between the hilus and GCL (Fig. 1A). Most Ki67+ cells formed clusters in the same region. When rats were fixed 3 days after the BrdU injection, most BrdU+ cells were found in the subgranular zone and innermost part of the GCL. Although BrdU+ cells were frequently located in clusters of Ki67+ cells, they were also found outside the clusters and were more dispersed than Ki67+ cells (Fig. 1A2). Proliferative Ki67+ cells and newly generated BrdU+ cells appear to be buried within the continuous plexus of PSA+ elements (Fig. 1A3–5). In this situation we could not determine how newly generated cells migrate from the proliferating sites and develop neurites.

For this reason, in the next experiments we used middle-aged rats with decreased numbers of newly generated cells BrdU+, Ki67+ proliferating cells and PSA+ immature+ cells, and there was nearly no continuous plexus consisting of PSA+ tangential processes (Fig. 1B–D). Therefore, we could easily observe the relationship among proliferative sites containing Ki67+ cells, newly generated BrdU-labeled cells, and developing PSA+ cells.

In older rats, a few masses of PSA+ developing cells were seen as patches (Fig. 1B–G). The majority of Ki67-positive cells (76%) formed clusters that contained 4.3 cells on average (Fig. 1B,C,E,G), although a small number of single Ki67+ cells and doublets were also observed. In the present experiment we regarded a cell aggregate of more than two cells as a cluster. At times, two clusters were in close proximity and appeared to be one huge cluster that contained ≈10–20 cells. Approximately half of the clusters of Ki67+ cells (48%) contained PSA+ cell bodies (Fig. 1B,E). Additionally, strongly PSA+ cells were very frequently seen in close proximity to clusters of Ki67+ cells and their tangential processes extended and penetrated the clusters or contacted the surface of the clusters (Fig. 1C–E,G). Consequently, the Ki67+ cells and PSA+ cells appeared to form a cluster. When the cluster cells expressed PSA strongly, they were mostly Ki67-negative (Fig. 1B,C), suggesting that they were postmitotic. However, weakly PSA+ cluster cells frequently exhibited Ki67 immunoreactivity (Figs. 1C,E2, 3B, 6C,D).

One day after the BrdU injection BrdU-labeled cells were seen in the SGZ and innermost part of the GCL (Fig. 1B). The majority of BrdU-labeled cells (81%) were found in clusters composed of Ki67+ cells and PSA+ cells (Figs. 1B, 2). Most BrdU-labeled cells (94%) inside the clusters were positive for Ki67 at 1 day after the BrdU injection.

Three days after the BrdU injection, half of the BrdU-labeled cells (56%) were still present in the clusters and frequently expressed Ki67 (73%), whereas the rest of the BrdU+ cells (44%) were located outside the clusters (Figs. 1C,E1–3, 2) and were almost negative for Ki67. The immunoreactive intensity varied in the BrdU-labeled cells. We found dot-like weak BrdU immunoreactivity in a substantial population of the BrdU+ cells (Fig. 1C5). This suggests that neural precursor cells divide a few times, in accordance with the reports of previous studies (Alvarez-Buylla and Lim, 2004; Kempermann et al., 2004a). A subpopulation of BrdU-labeled cells expressed PSA strongly and extended tangential and/or radial processes (Fig. 1D–F). In some cases, radial processes resembled dendrites of the granule cells (Fig. 1D2). This observation suggests that cells labeled with BrdU in the final cell division may develop dendrite-like processes as early as 3 days after the labeling.

Five to 7 days after the BrdU injection, most BrdU-labeled cells (80%) were present outside the clusters and dispersed around a cluster of Ki67+ cells, although a small population of the BrdU-labeled cells (20%) remained in the clusters (Figs. 1G, 2). There is a significant difference in the proportion of Ki67 cells inside and outside the clusters between 1 and 5–7 days after BrdU injection ($P < 0.0001$). Most of the BrdU-labeled cells were positive for PSA and had tangential and/or radial processes. At times they appeared to connect with clusters of Ki67+ cells through PSA+ tangential processes. Part of the BrdU-labeled PSA+ cells became granule-cell-like cells (data not shown), as has been shown in young adult rats (Seki, 2002b; Seki and Arai, 1993).

Analysis of the nature of cluster cells

In the subsequent experiments we explored developmental signals associated with the clusters and found very specific β-catenin expression in the SGZ and innermost part of the GCL (Fig. 3). The strong β-catenin expression was restricted mainly to cells forming clusters, although the weak ubiquitous expression was present throughout the entire hippocampus. β-Catenin expression was present in Ki67+/PSA+, Ki67+/PSA−, and Ki67−/PSA+ cells in the clusters, but was not found in Ki67+ cells in the hilus (Fig. 3A,B). The β-catenin expression of PSA+ cells outside clusters was mostly very low. Furthermore, the distribution pattern of strong β-catenin expression was found to almost completely coincide with that of strong N-cadherin expression in clusters (Fig. 3C), although weak ubiquitous N-cadherin expression was seen throughout the entire hippocampus. On a part of the plasma membrane of the cluster cells, β-catenin, N-cadherin, and PSA expressions appeared to coexist.

To examine the nature of proliferating cells, sections were immunostained with the antibodies for a neuronal marker, Hu, a proneuronal marker, MASH-1 (Kageyama et al., 1997; Okano and Darnell, 1997), and astrocytic markers, GFAP and S100β. Hu is known to be expressed by both immature and mature neurons (Okano and Darnell, 1997). It is generally difficult to count GFAP+/Ki67+ or GFAP+/BrdU+ cells because it is very hard to distinguish between GFAP+ cells and GFAP− cells surrounded by GFAP+ processes (Seki, 2002b; Shapiro et al., 2005). In this experiment, we counted Ki67+ cells that contained GFAP+ filaments in Hu+ cell bodies (Fig. 4A). This triple staining allows us to determine the number of GFAP+ cells more precisely than previously possible. Most Ki67+ proliferating cells express neuronal marker Hu (94%; Figs. 4A–C, 5) and the proneuronal marker MASH1 (88%; Fig. 4C,E). Hu expression in proliferating cells was much stronger in the cytoplasmic rim than in nuclei when compared with that in mature neurons. The subpopulation of Ki67+/Hu+ proliferating cells was strongly positive for GFAP (38%; Figs. 4A, 5) and Ki67+/Hu-/GFAP+ cells were rare (2%; Figs. 4F, 5). In the case of Ki67+/Hu-/

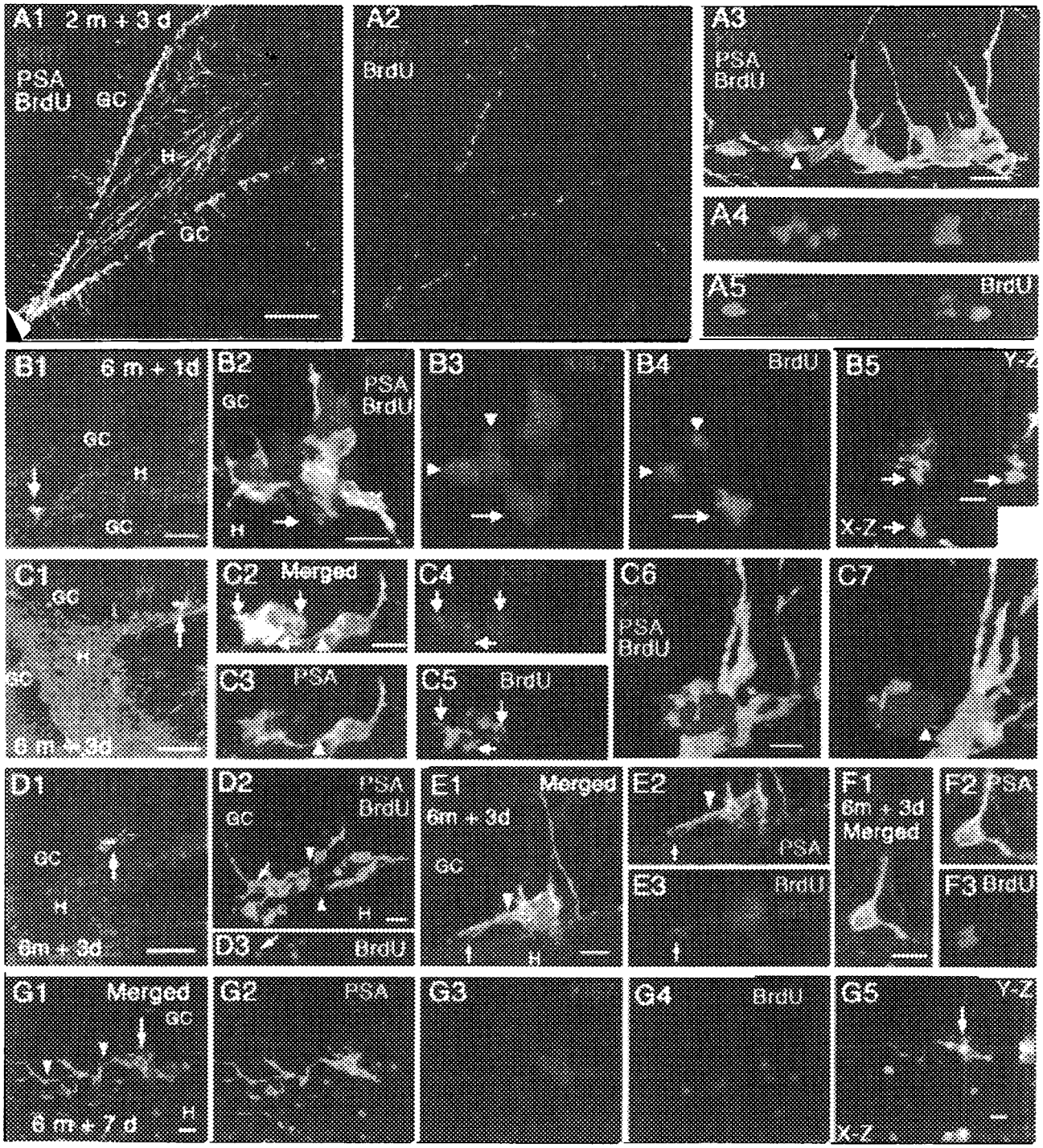

Fig. 1. Analysis of newly generated BrdU-labeled cells using a cell proliferation marker, Ki67, and an immature neuronal marker, PSA, in 2-month-old (A) and 6-month-old (B–G) rats. The number of PSA+ immature neurons was reduced in 6-month-old rats (B1,C1,D1) when compared with 2-month-old rats (A1). Three-dimensional images of A1–2, A3–5, B2–4, C6–7, D2, and G1–4 were reconstructed from 10, 11, 11, 11, 8, and 6 optical slices, respectively. Each image of A1–2, A3–5, B2–4, C2–5, D2–3, E1–3, F1–3, and G2–4 is obtained from the same optical sections with different filters. A: Many PSA+ immature+ neurons can be seen along the border of the GCL (GC) and hilus (H; A1). There are also Ki67+ proliferating cells and newly generated cells labeled by the BrdU that was injected into rats at 3 days before fixation (A1–5). The BrdU+ cells appear to be more dispersed than the Ki67+ cells (A2), suggesting that newly generated cells may migrate from proliferating sites. Ki67+ and BrdU+ cells appear to be buried in a plexus formed by PSA+ cells (A3). Note that PSA+ processes wind around Ki67+ and BrdU+ cells and are branched on them (arrowheads in A3). B–G: In 6-month-old rats BrdU was injected 1 (B), 3 (C–F), or 7 (G) days before fixation. Neurogenic regions are recognized as small patches consisting of Ki67+ proliferating cells, BrdU+ newly generated cells, PSA+ neuroblasts, and immature neurons (arrows in B1, C1, D1). The processes of PSA+ neuroblasts or immature neurons close to clusters appear to invade the clusters (arrowheads in C2–7 D2, E1, G1). Some BrdU-labeled cells are simultaneously positive for Ki67, suggesting that cells labeled 1–7 days ago are still in the cell cycle (arrows and arrowheads in B3,4 and arrows in C2,4,5, and orthogonal images of B5 and G5). Note that newly generated BrdU+/PSA+ cells give rise to radial (arrows in D2,3), tangential (arrows and arrowheads in E1–3) or both (F1–3) processes. Image C7 is obtained by 90° rotation of image C6 around the vertical axis to reveal the processes indicated by the arrowhead in C7. At 7 days after BrdU injection BrdU-labeled cells are distributed around a cluster of Ki67+ cells (G). Note radial and tangential PSA+ processes of newly generated BrdU+ cells are entangled. Scale bars = 100 μm in A1,B1,C1,D1; 10 μm in A3,B2,B5,C2,C6,D2,E1,F1,G1,G5.

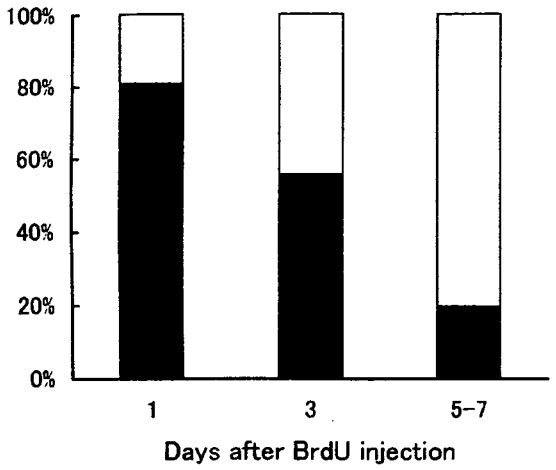

Fig. 2. The percentages of BrdU-labeled cells inside (black bars) or outside (gray bars) clusters of Ki67+ cells from 1 and to 5–7 days after BrdU injection. The percentage of the BrdU+ cells inside clusters is very high at 1 day after BrdU injection, but thereafter is decreased linearly between 1 and 7 days after BrdU injection, whereas the percentage of the BrdU+ cells outside clusters is increased. This indicates that cell proliferation occurs mainly in clusters and the developing cells migrate from the clusters to their surroundings.

GFAP+ cells of the SGZ the number might have been somewhat underestimated, since clear Hu+ cell bodies were not seen. Most Ki67+/Hu+ cells were very weakly positive for S100β (Fig. 4B). MASH-1 expression was confined to nuclei. The majority of MASH-1+ cells were also positive for Hu (68%; Fig. 4C–E) and the subpopulation was positive for GFAP (54%, Fig. 4D,E). At times we found Ki67+/Hu+/GFAP+ or MASH-1+/Hu+/GFAP+ cells with a radial process (Fig. 4A,E). These results indicate that most of the proliferating cells express neuronal markers, and the subpopulation expresses neuronal (or proneuronal) and astrocytic markers simultaneously.

Retrovirus analysis

To observe the fine morphology and intercellular relationship of newly generated cells, retrovirus-EGFP was directly injected into one location of the right and left dentate gyrus, and the rats were then fixed 2, 3, 4, and 5 days after the injection.

GFP expression in cells infected by retrovirus appeared by 2 days after the injection and were distributed within 200–400 μm of the injection site. Two days after the retrovirus injection 71% of GFP-labeled cells were found in clusters of Ki67+ cells. The average number of GFP-labeled cells within clusters was 2.45. There were two types of clusters of GFP+ cells: tangentially elongated

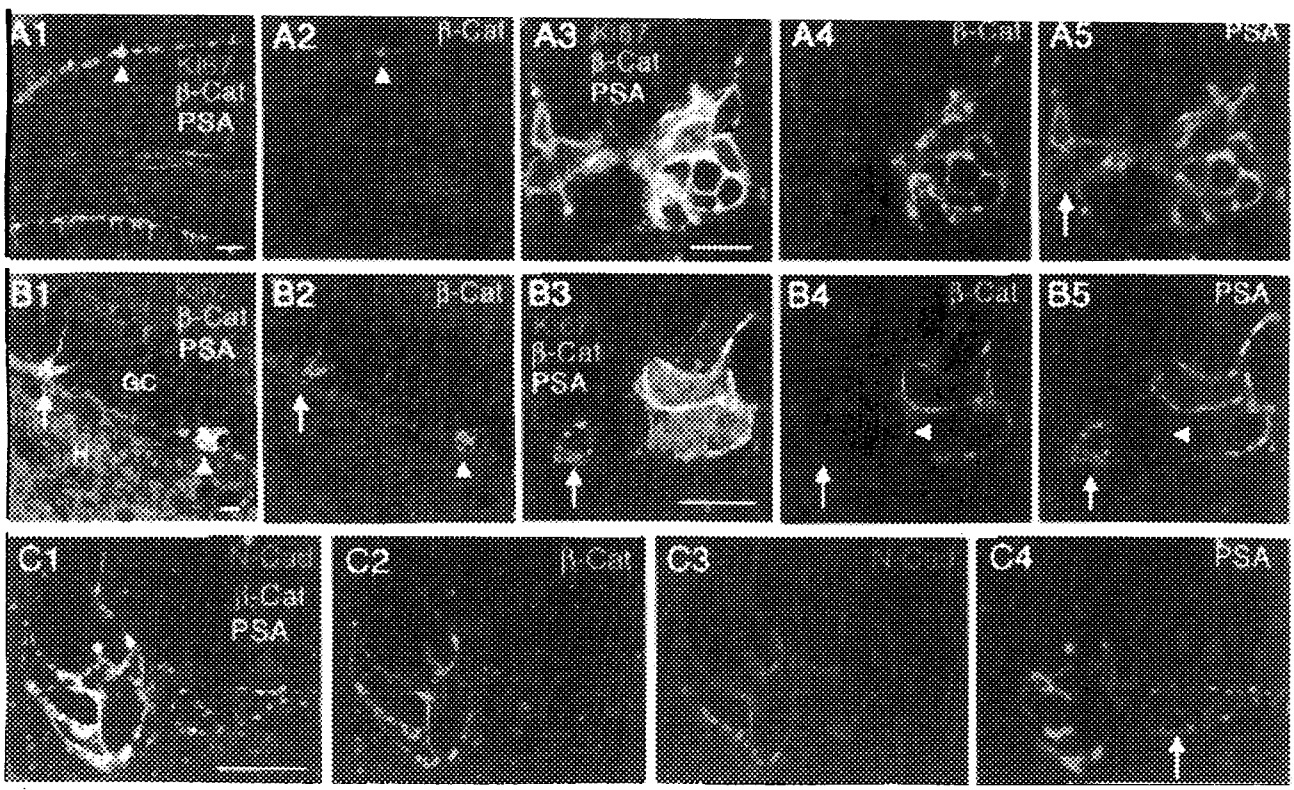

Fig. 3. Cluster cells express β-catenin and N-cadherin. Immunohistochemistry was performed in rats at the ages of 2 (**A,C**) and 6 (**B**) months. Clusters pointed by arrowheads in A1 and B1 are enlarged in A3–5 and B3–5, respectively. Strong β-catenin expression is mainly found in cluster cells consisting of Ki67+ proliferating/PSA+ or Ki67+/PSA− cells, and postmitotic PSA+ cells (arrows and arrowheads in A,B). β-Catenin expression almost completely coincides with N-cadherin expression (C). Note that not all β-catenin expression is associated with PSA+ cells (arrowheads in B4,5), particularly those outside clusters (arrows in A5, B3–5, C4). GC, granule cell layer; H, hilus. Scale bars = 100 μm in A1; 50 μm in B1; 10 μm in A3,B3.

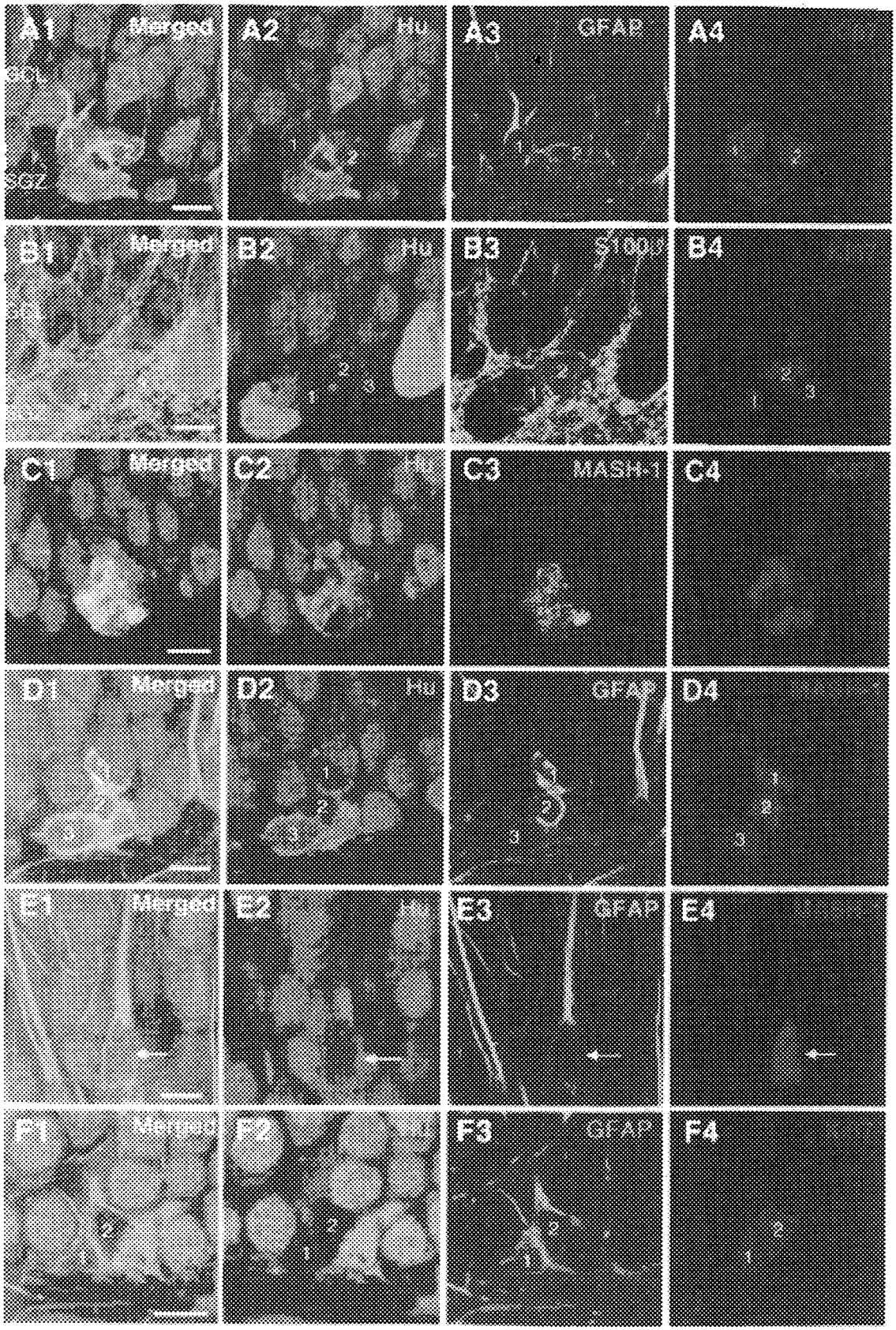

Fig. 4. Nature of Ki67+ proliferating cells. Single sections were immunostained with several antibodies (as indicated) and were observed with different filters. The same numbers in cells (**A,B,D,F**) or arrows (**E**) indicate the same cells. Most Ki67+ proliferating cells express neuronal marker Hu (A,B) or proneuronal marker MASH1 (**C**). Some Ki67+/Hu+ cells are simultaneously positive for GFAP (1, 2 in A, 1 in F) and very weakly positive for S100β (1, 2, 3 in B). Ki67+/GFAP+/Hu− cells are rare (2 in F). The majority of MASH1+ cells are also positive for Ki67 and express both Hu and GFAP (1, 2 in D and arrow in E). Note that Hu expression is stronger in the cytoplasmic rim than in the nuclei (A–F), and that cells with a radial process express both Hu and GFAP (1 in A and arrow in E). Scale bars = 10 μm.

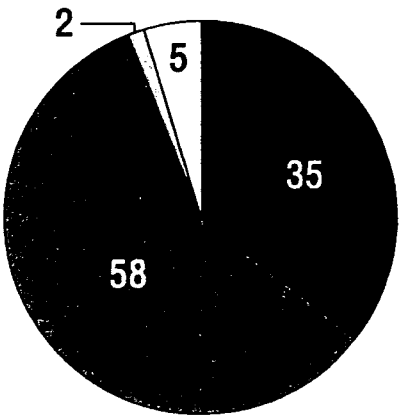

Fig. 5. Composition of Ki67+ proliferating cells in the GCL and SGZ of the dentate gyrus. The hippocampal section was immunostained for Ki67, Hu, and GFAP (Black, Ki67+/Hu+/GFAP+; dark gray, Ki67+/Hu+/GFAP−; light gray, Ki67+/Hu−/GFAP+; white, Ki67+/Hu−/GFAP−). The number indicates the percentage of immunoreactive cells. Most of the Ki67+ proliferating cells express a neuronal marker, Hu, and one-third express Hu and GFAP.

clusters under the GCL or SGZ (Fig. 6A) and radially elongated clusters that invade the innermost part of the GCL (a similar type of cluster in Fig. 6B,C). Various types of GFP-labeled cells were found: cells with short processes forming a cluster or doublet (71%), cells with tangentially oriented long processes (10%), cells with radially oriented long processes (3%), and single cells with short and fine processes (16%; Figs. 6A, 8). Other than these cells, cells with long fine multipolar processes were observed, particularly in great numbers near the injection sites, and these appeared to be inflammatory reactive glial cells. We did not count these cells.

Three days after the retrovirus injection the number of GFP-labeled cells had increased and the percentages of types of GFP-labeled cells were as follows: cells with short processes forming a cluster or doublet (55%), cells with tangentially oriented long processes (15%), cells with radially oriented long processes (3%), and single cells with short and fine processes (27%; Figs. 6B,C, 7A–C, 8). A process that was more than double the length of the long axis of the cell body was regarded as long. Clusters that were elongated radially or tangentially contained 2–8 cells (Fig. 6B,C and a similar type of cluster in Fig. 6A). The average number of GFP-labeled cells within a cluster was 4.43. The majority of the GFP-labeled cells in the clusters expressed Ki67 (52%) and Hu (90%), and 88% of the Ki67+/GFP+ cells expressed Hu. Some GFP+/Ki67+/Hu+ cells in radially elongated clusters had radially oriented processes (Fig. 6C1,2). A subpopulation of the GFP+/Ki67+ cells also expressed PSA, although PSA immunoreactivity was weaker in Ki67+ than Ki67− cells (Fig. 6C). In a rare case, dividing PSA+ cells were found, supporting the notion that some of the PSA+ cells are proliferative precursor cells (Fig. 6D). GPF+/Hu+ cells in clusters had GFAP+ filaments that sometimes formed circles (Fig. 6E). A subpopulation of GFP+/Ki67+/Hu+ cells gave rise to short processes that engulfed neighboring cells (Fig. 7A). Outside the clusters, most of the GFP+ cells were negative for Ki67 and had tangential processes that very frequently made contact with Ki67+ cell clusters (Fig. 7B,C).

Four days after the retrovirus injection, cells forming clusters had decreased in number (13%) and the majority of the GFP-labeled cells had tangentially (59%) or radially (14%) oriented processes or both (7%; Figs. 7D–G, 8). There are significant differences in the proportions of cluster cells to noncluster cells ($P < 0.0001$) and tangential cells to nontangential cells ($P < 0.0001$) between 2 and 4 days after retrovirus injection. Most of the GFP+ cells outside the Ki67+ cell clusters were negative for Ki67 and had tangential or radial processes. One of the tangential processes arising from the GFP+ cells frequently made contact with Ki67+ proliferating cells (Fig. 7D,F). Some GFP+/Ki67− cells with a radial process lay at the center of the clusters and gave rise to long tangential processes in addition to the radial process (Fig. 7E). In both cases the processes were branched at the sites of contact with the clusters of Ki67+ cells and appeared to surround the Ki67+ proliferating cells (Fig. 7D,E). Additionally, at 5 days after the retrovirus injection we found GFP+ cells with tangential and radial processes, both of which made contact with Ki67+ proliferating cells (Fig. 7H). Most of the radial processes were fine, and arose mainly from GFP+ cell bodies or partly from tangential processes. A minor portion of the radial processes was thick, had fine stick-like processes, and resembled developing dendrites of the dentate granule cells (Fig. 7G). The increase in GFP+ cells with tangential processes preceded that in GFP cells with radial processes, suggesting that newly generated cells develop tangential processes first and then radial processes (Fig. 8). Our previous study has shown that most of the GFP-labeled cells become typical granule cells 30 days after retrovirus injection (Tanaka et al., 2004).

Time-lapse imaging

The in vivo analysis of BrdU/Ki67/PSA labeling and retrovirus-GFP labeling suggested the possibility that newly generated cells with tangential processes first migrate tangentially and then extend radial processes during the course of granule cell development. To observe the developmental course directly we performed time-lapse imaging in slice culture of the hippocampus from P8 rats that were injected with retrovirus bearing the GFP gene into the dentate regions at P5. As previously reported (Namba et al., 2005), during the early postnatal period neurogenesis occurs predominantly in the hilus and partially in the SGZ, whereas in adults neurogenesis occurs exclusively in the SGZ. Because postnatal neurogenesis in the SGZ continues from the early postnatal to adult stages, we assume that adult-type neurogenesis occurs in the SGZ of the early postnatal dentate gyrus.

In agreement with the previous in vivo experiments (Namba et al., 2005), GFP-labeled cells were found mainly in the hilus and partially in the SGZ of the cultured hippocampal slices. We observed the SGZ of 40 hippocampal slices over 24 hours and found 10 cells migrating tangentially and 11 cells involved in neurite development. GFP-labeled cells possessing tangentially oriented leading and trailing processes migrated tangentially through the SGZ (Fig. 9A). Although the trailing processes of the neuroblasts sometimes became very thin during their migration, the tip seemed to be left behind. Additionally, we observed radially migrating neuroblasts. However, it was

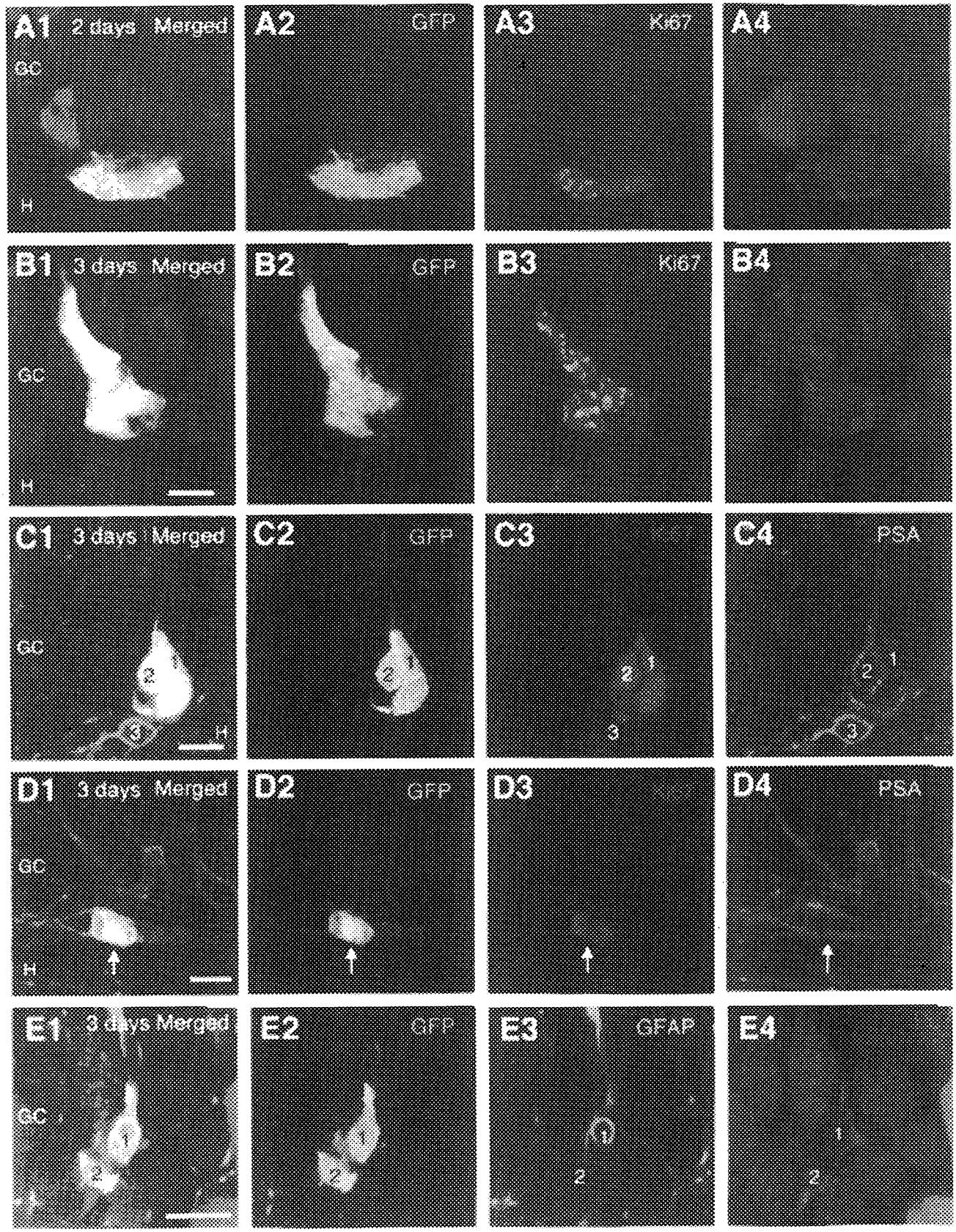
A1 2 days Merged
GC
H
A2 GFP
A3 Ki67
A4
B1 3 days Merged
GC
H
B2 GFP
B3 Ki67
B4
C1 3 days Merged
GC
2
3
H
C2 GFP
C3
2 1
3
C4 PSA
2 1
3
D1 3 days Merged
GC
H
D2 GFP
D3
D4 PSA
E1 3 days Merged
GC
1
2
E2 GFP
1
2
E3 GFAP
1
2
E4
1
2

Figure 6

difficult to determine whether the GFP+ cells migrated just within the GCL (putative adult-type migration) or from the hilus to the GCL (putative early postnatal-type migration), because most of the GFP+ progenitor cells were present in the hilus and migrated radially to the GCL during early postnatal period (Namba et al., 2005).

In another case, GFP-labeled cells exhibited shortening of their tangential processes and then gave rise to a very thin radial process. When the thin radial process developed, the cells still possessed the short tangential process. Subsequently, the radial process gradually became thick, branched, and finally developed into dendrite-like radial processes (Fig. 9). The results of the present time-lapse imaging experiments show that at least a subpopulation of neuroblasts actually migrates tangentially and then extends apical dendrites. These results support the above-mentioned interpretation of the in vivo data.

DISCUSSION

The present data show that in the adult hippocampal neurogenic region, proliferative neural precursors and postmitotic neuroblasts form clusters whose cells express cell adhesion molecules, such as N-cadherin/catenin and PSA. They also show that the postmitotic neuroblasts move tangentially from the cell proliferation site, leaving trailing processes behind at the proliferation site, which is followed finally by extension of radially oriented dendrites. The present results suggest that a systematic cellular arrangement and intercellular interaction of proliferating cells and neuroblasts exist in adult hippocampal neurogenesis.

Clustering

Although several recent reports have described that proliferating cells make clusters in the SGZ of the hippocampus (Palmer et al., 2000; Seki, 2002b; Seri et al., 2004), the intercellular relationship of the cellular components forming clusters in the hippocampus have not been fully understood. The present BrdU/Ki67 and retrovirus-GFP analysis indicate that proliferating cells form clusters together with postmitotic neuroblasts, and that Hu+ proliferating cells within clusters sometimes engulf neighboring cells by their short processes (Fig. 7A). In this regard, it has previously been reported that GFAP+ cells also surround or engulf neighboring neuroblasts (Palmer et al., 2000; Seki, 2002b; Seri et al., 2004; Shapiro et al., 2005). Thus, various types of cells within clusters can interact on the surfaces of apposed cells.

Furthermore, strong β-catenin and N-cadherin expression were seen exclusively in the cells inside clusters, and coexisted on the plasma membrane of the cluster cells. Additionally, PSA was found to colocalize partially with β-catenin. It is well known that PSA modulates the cell adhesion mediated by NCAM, L1, and cadherin (Rutishauser and Landmesser, 1996; Fujimoto et al., 2001), whereas β-catenin enhances cadherin-mediated cell adhesion (Takeichi and Abe, 2005). PSA is also reported to facilitate cell migration in the subventricular zone (Ono et al., 1994) and enhance neurite formation (Rutishauser and Landmesser, 1996). Thus, the balance between PSA and N-cadherin/β-catenin expressions may be involved in the regulation of cell proliferation, differentiation, and migration (Rutishauser and Landmesser, 1996; Nelson and Nusse, 2004; Petridis et al., 2004).

Additionally, β-catenin has been known as a key component of the Wnt signaling pathway (Nelson and Nusse, 2004). Wnt families are shown to be expressed by cells in the inner border of the GCL (Shimogori et al., 2004) and to be involved in adult neurogenesis (Madsen et al., 2003; Lie et al., 2005). Thus, it is also possible that both the Wnt and N-cadherin pathways play a role in adult neurogenic events within the clusters.

Nature of cluster cells

Most of the proliferating cells expressed a neuronal marker, Hu, and a proneuronal marker, MASH-1. This suggests that most proliferative precursor cells are committed to the neuronal cell lineage. Similarly, proliferative Hu+ neuronal precursors have been reported in the embryonic neocortex (Miyata et al., 2004) and early postnatal hippocampus (Namba et al., 2005). Furthermore, one-third of the proliferating cells were double-labeled for both Hu and GFAP or MASH-1 and GFAP. Because primary neural precursor cells are known to express GFAP (Seri et al., 2001; Filippov et al., 2003; Fukuda et al., 2003; Garcia et al., 2004; Kempermann et al., 2004a), the Hu+/GFAP+ and MASH-1+/GFAP+ cells could represent an intermediate state when proliferative GFAP+ cells change into proliferative Hu+ neuronal precursor cells. Similar intermediate cells have also been found in the postnatal dentate gyrus (Namba et al., 2005).

Furthermore, some of the Hu+/GFAP+ and MASH-1+/GFAP+ cells had a radial process. In this respect, GFAP+ radial cells (or radial glial cells) were previously considered to be primary precursor cells and are negative for markers such as DCX (Kempermann et al., 2004a). Since the present results suggest that at least the subpopulation of GFAP+ radial cells has already been committed to the neuronal cell lineage, the identity of the GFAP+ radial cells should be reconsidered.

Migration and neurite formation

Several reports have described immature granule cells with long tangential processes in the adult dentate GCL in normal and epileptic rats (Seress and Mrzljak, 1987; Spigelman et al., 1998; Nacher et al., 2001; Seki, 2002b; Dashtipour et al., 2002; Jones et al., 2003; Ribak et al., 2004; Seri et al., 2004; Shapiro and Ribak, 2005; Esposito et al., 2005). Further, recent electrophysiological studies have shown proliferative precursor cells with short tangential processes (van Praag et al., 2002; Fukuda et al.,

Fig. 6. Retrovirus-GFP analysis demonstrating the detailed morphology of newly generated cells in clusters. Newly generated cells were labeled with retrovirus-GFP at 2 (A) or 3 (B–E) days before fixation. A: A tangentially elongated cell cluster is located under the GCL or the SGZ. Note that Hu expression in GFP+ cells is stronger in the cytoplasmic rim than in the nuclei (A,B,E). B: A radially elongated cell cluster has invaded the innermost area of the GCL. Most GFP-labeled cells are positive for Ki67 (A–D) and Hu (A,B,E), suggesting that they are still in the cell cycle and have already been committed to the neuronal lineage. C: A subpopulation of the Ki67+ proliferating cells expresses PSA (2, the same numbers in cells indicate the same cells). Note that not all GFP+/Ki67+ cells express PSA (1) and a strongly PSA expressing cell (3) associated with a cell cluster withdraws from the cell cycle. D: GFP-labeled cells expressing PSA are dividing. E: A GPF+/Hu+ cell in a cluster have GFAP+ filaments that forms circles (1). GC, granule cell layer; H, hilus. Scale bars = 10 μm.

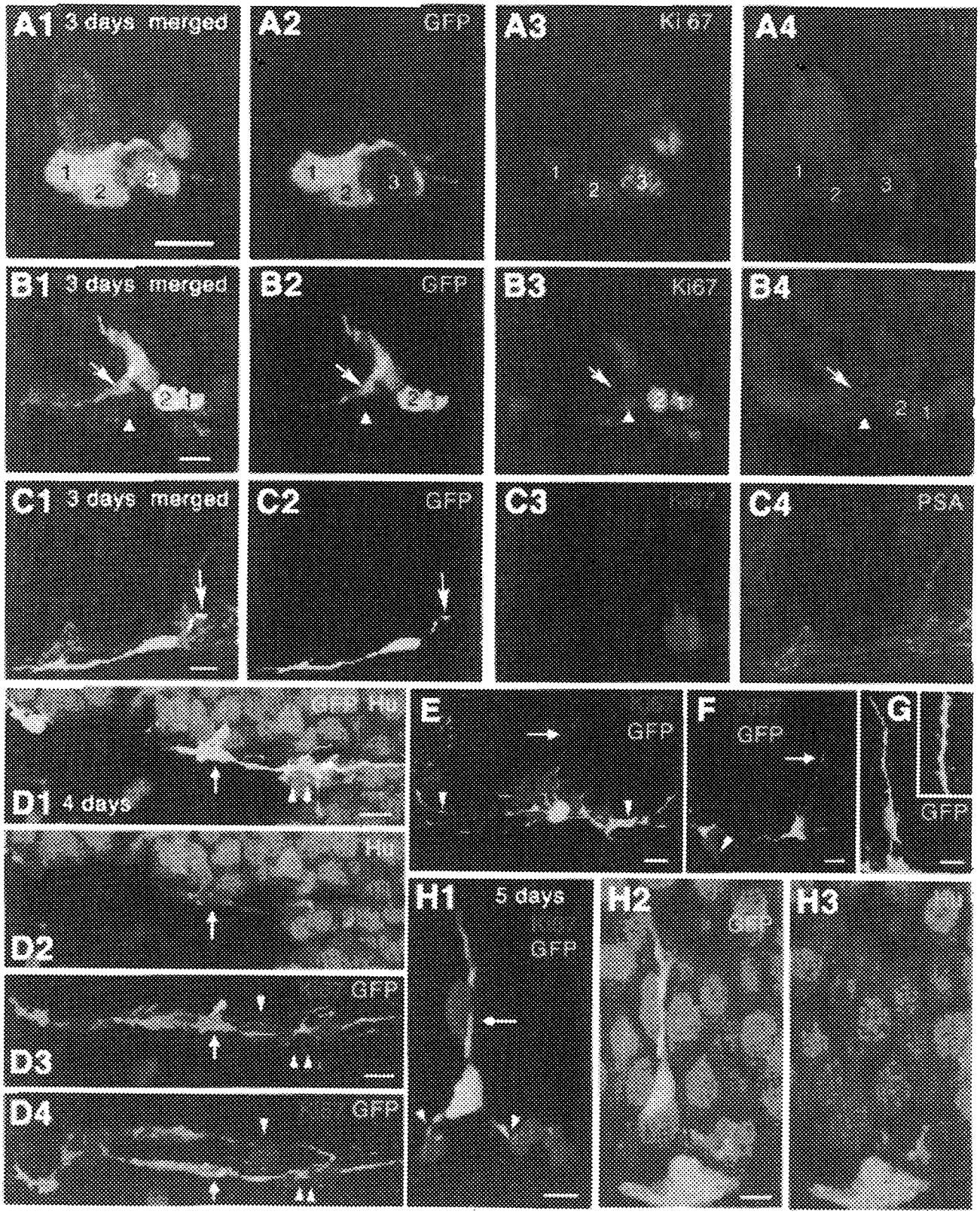
A1 3 days merged
A2 GFP
A3 Ki 67
A4
B1 3 days merged
B2 GFP
B3 Ki67
B4
C1 3 days merged
C2 GFP
C3
C4 PSA
D1 4 days
D2
D3 GFP
D4 GFP
E GFP
F GFP
G GFP
H1 5 days GFP
H2 GFP
H3

Figure 7

2003; Kempermann et al., 2004a; Alvarez-Buylla and Lim, 2004; Esposito et al., 2005; Tozuka et al., 2005). Yet the questions remain about when the long or short tangential processes appear during the developmental course and whether or not these cells with tangential processes migrate tangentially.

The present quantitative data of BrdU/Ki67 labeling and retrovirus labeling indicate that during the developmental course proliferating cells inside clusters have short tangential processes, and when postmitotic cells withdraw from the proliferative site they extend long tangential processes. Furthermore, these in vivo experiments and in vitro time-lapse imaging of early postnatal hippocampal slices showed that the cells with long tangential processes migrated tangentially, then their tangential processes shortened and began to extend thin radial processes that become apical dendritic processes. The present study, however, does not preclude any other migration pattern, such as oblique or radial migration. A radially elongated shape of cell clusters suggests that newly generated cells migrate radially at a short distance within the clusters. In time-lapse imaging of early postnatal hippocampal slices, some GFP+ neuroblasts were found to migrate radially in the GCL. However, a higher incidence of the tangentially oriented neuroblasts in the in vivo analysis of the adult dentate gyrus suggests that most of the neuroblasts migrate tangentially and the minority migrates with a different pattern. There may also be some difference in radial migration between the early postnatal and adult dentate gyrus.

During the tangential migration the migrating cells appeared to leave a tangential process behind in the clusters. In this regard, it is worth noting that similar intercellular relationships have so far been well studied in the developing neocortex where the neuroblasts migrate along radial glial processes (Rakic, 1971, 2003; Marin-Padilla, 1998; Miyata et al., 2001; Tamamaki et al., 2001; Gaiano and Fishell, 2002; Fujita, 2003; Tabata and Nakajima, 2003; Noctor et al., 2004; Ever and Gaiano, 2005). Recently, radial glial cells have been demonstrated to be neural progenitor cells (Miyata et al., 2001; Tamamaki et al., 2001; Noctor et al., 2004), which also means that proliferative neural progenitor cells and migrating neuroblasts make contact with each other. These intercellular relationships between proliferating cells and migrating neuroblasts suggest that embryonic and adult neurogenesis may share similar mechanisms in neuronal development.

In summary, the present analysis shows how neural precursor cells proliferate, migrate, and extend their neuronal processes (Fig. 10). Cell proliferation primarily occurs in clusters where proliferating cells and postmitotic neuroblasts express N-cadherin/β-catenin and PSA. They are in close contact with each other and extend short processes that sometimes engulf neighboring cells. During the developmental stages the nature of the neural precursor cells in the clusters could change as follows: Ki67+/GFAP+/β-catenin+/N-cadherin+, Ki67+/GFAP+/β-catenin+/N-cadherin+/Hu+, Ki67+/β-catenin+/N-cadherin+/Hu+, Ki67+/β-catenin+/N-cadherin+/Hu+/PSA+, and β-catenin+/N-cadherin+/Hu+/PSA+ cells. However, the proliferation of precursors outside the clusters to a small extent cannot be excluded. When postmi-

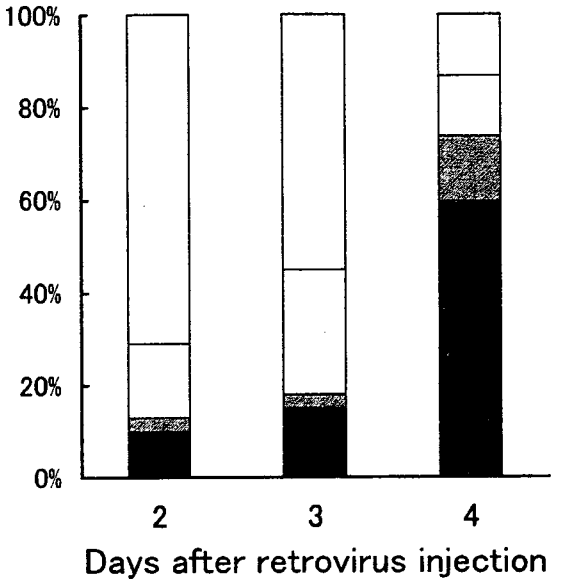

Fig. 8. Change in the cluster and morphology of GFP+ cells during development. At 2 days after the retrovirus injection, a majority of GFP+ cells form clusters (white bars). This type of GFP+ cell rapidly decreases in percentage during development, whereas GFP cells with tangential (black bars) or radial (dark gray bars) processes increase. GFP+ cells with short processes or without processes are indicated by light gray bars. Note that GFP cells with a radial processes increase later than GFP+ cells with tangential processes, suggesting that newly generated cells may develop tangential processes first and then a radial process.

Fig. 7. Neurite formation of the newly generated cells that were labeled with retrovirus-EGFP at 3 (**A–C**) 4 (**D–G**) or 5 (**E**) days before fixation. The same number in cells (A,B), the arrows or arrowheads (C–H) indicate the same cells. A: In a cluster of Ki67+/Hu+ cells, two cells labeled with GFP (1, 2) extend short processes that engulf a neighboring cell (3). Note that Ki67+ cells make contact with a large Hu+ cell. B: GFP+/Hu+ cells form a cluster. Most of the cells express Ki67 (arrowhead, 1 and 2), but one cell is devoid of Ki67 (arrow), suggesting that the latter cell has withdrawn from the cell cycle. The postmitotic cell (arrow) gives rise to a tangentially oriented process and seems to migrate from the cluster. C: A GFP+ postmitotic cell gives rise to tangentially oriented processes. The left and the right processes appear to be a leading and a trailing process, respectively, and the right one makes contact with a cluster of Ki67+ cells (arrow). The GFP+ cell appears to express PSA weakly. D: A postmitotic GFP+/Hu+ cell (arrow) tangentially extends an oriented process that makes contact with Ki67+ proliferating cells; it branches there and give rise to fine processes (double arrowheads in D1, 3, 4). The image D4 is obtained by 90° rotation of image D3 around the horizontal axis to reveal the contacts between the GFP+ fine processes and Ki67+ proliferating cells (single arrowheads and double arrowheads in D3, 4). E: A GFP+ cells in a cluster of Ki67+ cells extends radial (arrow) and tangential (arrowhead) processes. F: A GFP+ cell has both radial and tangential processes, with the tip of the latter appearing to reach a Ki67+ cell cluster (arrowhead). G: A GFP+ cells at an advanced developmental stage extend a dendrite-like radial process that has a small spine-like protrusion. The inset shows a higher magnification image of the radial process. **H:** A postmitotic GFP+/Hu+ cell extends apical (arrow in H1) and basal processes (arrowheads in H1), both of which make contact with Ki67 cells. Three-dimensional images of D2–3, E, F, G, H1 were reconstructed from 11, 12, 8, 17, and 16 optical slices, respectively. GC, granule cell layer; H, hilus. Scale bars = 10 μm.

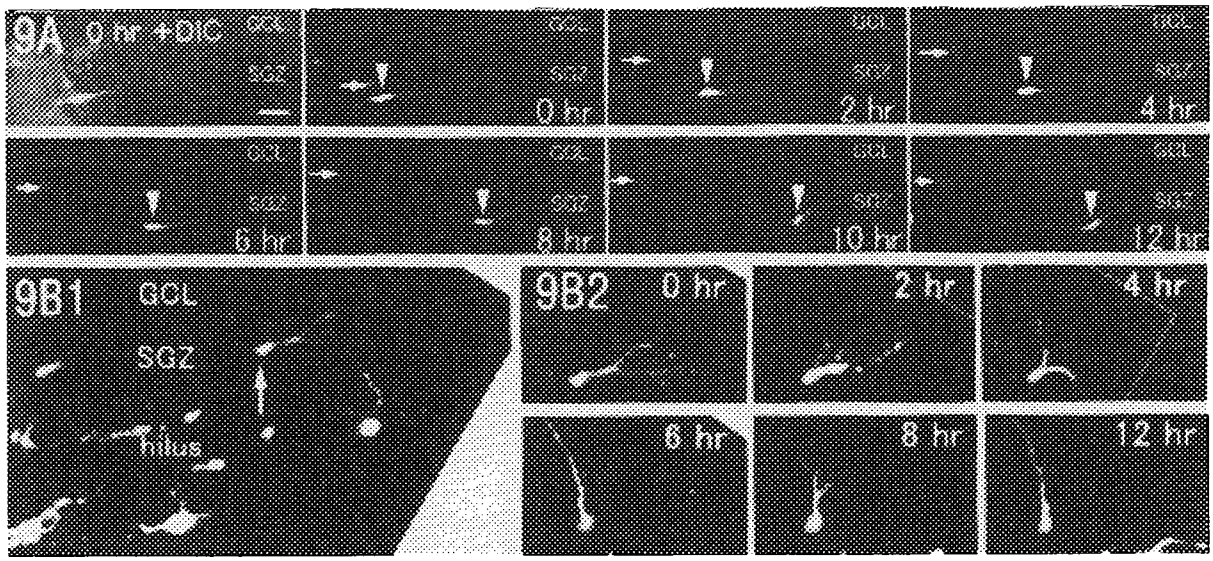

Fig. 9. Time-lapse imaging of the development of GFP-labeled cells in slice culture from postnatal day 8 (P8) rats that were injected with retrovirus bearing GFP gene into the dentate regions at P5. **A:** A tangentially oriented GFP-labeled cell has migrated tangentially. The upper left image shows a projection image of confocal laser scanning microscopy and differential interference contrast (DIC) microscopy after 0 hours in culture. The lighter area indicates the GCL. The migrating cell (arrowhead) has tangentially oriented leading and trailing processes, the latter of which appears to have become very thin after 6–10 hours in culture and somewhat thicker after 12 hours. The arrow indicates radially oriented cells that migrate a short distance radially. **B:** A tangentially oriented GFP-labeled cell whose tangential processes have shortened and given rise to new thin radial processes can be seen. The thin radial processes are developing into thick dendrite-like processes. The position of the GFP-labeled cell in the dentate gyrus is indicated by the arrow in 9B1. Scale bar = 20 μm.

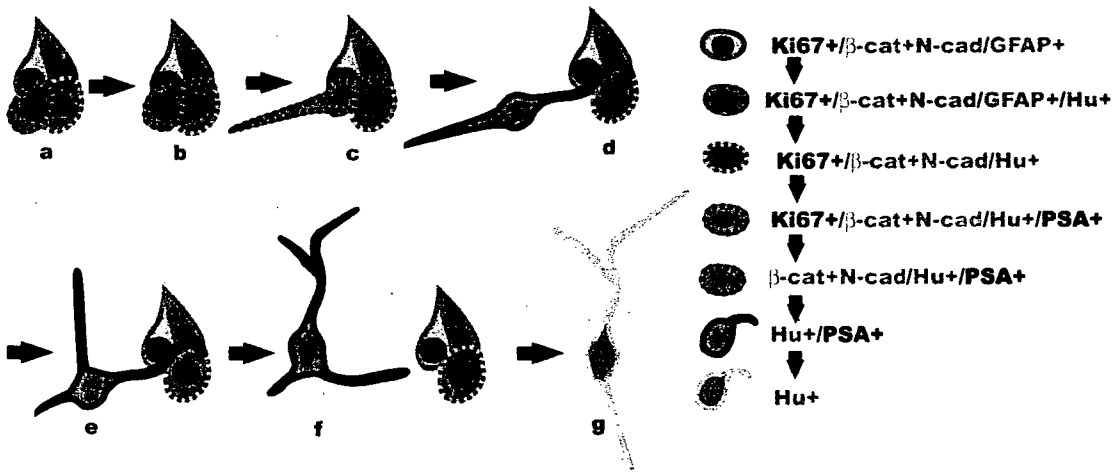

Fig. 10. Hypothetical model of cell clustering, migration, and neurite formation in adult hippocampal neurogenesis. (a) Proliferating cells are forming clusters. Most proliferating cells in the cluster express Hu, an immature and mature neuronal marker, and the subset expresses PSA, an immature neuronal marker. These cells inside clusters specifically express β-catenin (β-cat) and N-cadherin (N-cad). (b) In the cluster newly generated cells often extend short processes that engulf neighboring cells. (c) Postmitotic cells remain in the clusters during a certain period. Consequently, the clusters contain both Ki67+ proliferating cells and PSA+ postmitotic neuroblasts, both of which express β-catenin and N-cadherin. (d) When the newly generated cells withdraw from the clusters, they lose their strong β-catenin and N-cadherin expression, and PSA expression is increased. Then they migrate mainly tangentially, extending tangentially oriented processes; one of these processes is left behind within the clusters. (e) The tangential neuroblasts begin to extend radial processes. However, they still have basal dendrites that sometimes make contact with the clusters. (f) The radial processes develop into dendrites of the granule cells. (g) Finally, the neuroblasts develop into mature granule cells and lose their PSA expression. The systematic cellular arrangement and intercellular relationship may function as a favorable environment that supports neurogenesis in adult neural tissue.

totic neuroblasts withdraw from the clusters, β-catenin and N-cadherin expressions are downregulated and PSA expression is upregulated. PSA+ postmitotic neuroblasts migrate mainly tangentially from the clusters, extending their tangentially oriented long processes, one of which often retains contact with the proliferative site. These

close intercellular relationships via these cell adhesion molecules may play a functional role in the signaling of adult hippocampal neurogenesis. Next, the neuroblasts shorten their tangential processes and begin to extend thin radial processes that become apical dendritic processes similar to those of the granule cells. These observations suggest that adult hippocampal neurogenesis has a systematic cellular arrangement and intercellular association. In the adult hippocampus, proliferating neural progenitor cells are surrounded by adult tissue that seems to be an inappropriate environment for neurogenesis, as has been described in transplantation experiments (Suhonen et al., 1996; Shihabuddin et al., 2000; Seki, 2003). The systematic cellular arrangement and intercellular relationship may function as a favorable environment that supports neurogenesis in adult neural tissue.

ACKNOWLEDGMENTS

We thank Drs. Hirotaka J. Okano (Keio University) and Robert B. Darnell (Rockefeller University) for anti-Hu antibody and Dr. Nobuaki Tamamaki (Kumamoto University) for anti-GFP antibody. We thank Drs. Akiko Nishiyama (University of Connecticut) and Alison Murray for reading and editing the manuscript.

LITERATURE CITED

Abrous DN, Koehl M, Le Moal M. 2005. Adult neurogenesis: from precursors to network and physiology. Physiol Rev 85:523–569.

Altman J, Das GD. 1965. Autoradiographic and histological evidence of postnatal hippocampal neurogenesis in rats. J Comp Neurol 124:319–335.

Alvarez-Buylla A, Lim DA. 2004. For the long run: maintaining germinal niches in the adult brain. Neuron 41:683–686.

Cameron HA, Woolley CS, McEwen BS, Gould E. 1993. Differentiation of newly born neurons and glia in the dentate gyrus of the adult rat. Neuroscience 56:337–344.

Dashtipour K, Yan XX, Dinh TT, Okazaki MM, Nadler JV, Ribak CE. 2002. Quantitative and morphological analysis of dentate granule cells with recurrent basal dendrites from normal and epileptic rats. Hippocampus 12:235–244.

Doetsch F. 2003. A niche for adult neural stem cells. Curr Opin Genet Dev 13:543–550.

Doetsch F, Hen R. 2005. Young and excitable: the function of new neurons in the adult mammalian brain. Curr Opin Neurobiol 15:121–128.

Esposito MS, Piatti VC, Laplagne DA, Morgenstern NA, Ferrari CC, Pitossi FJ, Schinder AF. 2005. Neuronal differentiation in the adult hippocampus recapitulates embryonic development. J Neurosci 25: 10074–10086.

Ever L, Gaiano N. 2005. Radial 'glial' progenitors: neurogenesis and signaling. Curr Opin Neurobiol 15:29–33.

Filippov V, Kronenberg G, Pivneva T, Reuter K, Steiner B, Wang LP, Yamaguchi M, Kettenmann H, Kempermann G. 2003. Subpopulation of nestin-expressing progenitor cells in the adult murine hippocampus shows electrophysiological and morphological characteristics of astrocytes. Mol Cell Neurosci 23:373–382.

Fujimoto I, Bruses JL, Rutishauser U. 2001. Regulation of cell adhesion by polysialic acid. Effects on cadherin, immunoglobulin cell adhesion molecule, and integrin function and independence from neural cell adhesion molecule binding or signaling activity. J Biol Chem 276:31745–31751.

Fujita S. 2003. The discovery of the matrix cell, the identification of the multipotent neural stem cell and the development of the central nervous system. Cell Struct Funct 28:205–228.

Fukuda S, Kato F, Tozuka Y, Yamaguchi M, Miyamoto Y, Hisatsune T. 2003. Two distinct subpopulations of nestin-positive cells in adult mouse dentate gyrus. J Neurosci 23:9357–9366.

Gaiano N, Fishell G. 2002. The role of notch in promoting glial and neural stem cell fates. Annu Rev Neurosci 25:471–490.

Garcia AD, Doan NB, Imura T, Bush TG, Sofroniew MV. 2004. GFAP-expressing progenitors are the principal source of constitutive neurogenesis in adult mouse forebrain. Nat Neurosci 7:1233–1241.

Gould E, Gross CG. 2002. Neurogenesis in adult mammals: some progress and problems. J Neurosci 22:619–623.

Jones SP, Rahimi O, O'Boyle MP, Diaz DL, Claiborne BJ. 2003. Maturation of granule cell dendrites after mossy fiber arrival in hippocampal field CA3. Hippocampus 13:413–427.

Kageyama R, Ishibashi M, Takebayashi K, Tomita K. 1997. bHLH transcription factors and mammalian neuronal differentiation. Int J Biochem Cell Biol 29:1389–1399.

Kaplan MS, Hinds JW. 1977. Neurogenesis in the adult rat: electron microscopic analysis of light radioautographs. Science 197:1092–1094.

Kempermann G, Jessberger S, Steiner B, Kronenberg G. 2004a. Milestones of neuronal development in the adult hippocampus. Trends Neurosci 27:447–452.

Kempermann G, Wiskott L, Gage FH. 2004b. Functional significance of adult neurogenesis. Curr Opin Neurobiol 14:186–191.

Key G, Petersen JL, Becker MH, Duchrow M, Schluter C, Askaa J, Gerdes J. 1993. New antiserum against Ki-67 antigen suitable for double immunostaining of paraffin wax sections. J Clin Pathol 46:1080–1084.

Kosaka T, Hama K. 1986. Three-dimensional structure of astrocytes in the rat dentate gyrus. J Comp Neurol 249:242–260.

Kuhn HG, Dickinson-Anson H, Gage FH. 1996. Neurogenesis in the dentate gyrus of the adult rat: age-related decrease of neuronal progenitor proliferation. J Neurosci 16:2027–2033.

Lie DC, Colamarino SA, Song HJ, Desire L, Mira H, Consiglio A, Lein ES, Jessberger S, Lansford H, Dearie AR, Gage FH. 2005. Wnt signalling regulates adult hippocampal neurogenesis. Nature 437:1370–1375.

Madsen TM, Newton SS, Eaton ME, Russell DS, Duman RS. 2003. Chronic electroconvulsive seizure up-regulates beta-catenin expression in rat hippocampus: role in adult neurogenesis. Biol Psychiatry 54:1006–1014.

Marin-Padilla M. 1998. Cajal-Retzius cells and the development of the neocortex. Trends Neurosci 21:64–71.

Mercier F, Kitasako JT, Hatton GI. 2002. Anatomy of the brain neurogenic zones revisited: fractones and the fibroblast/macrophage network. J Comp Neurol 451:170–188.

Miyata T, Kawaguchi A, Okano H, Ogawa M. 2001. Asymmetric inheritance of radial glial fibers by cortical neurons. Neuron 31:727–741.

Miyata T, Kawaguchi A, Saito K, Kawano M, Muto T, Ogawa M. 2004. Asymmetric production of surface-dividing and non-surface-dividing cortical progenitor cells. Development 131:3133–3145.

Nacher J, Crespo C, McEwen BS. 2001. Doublecortin expression in the adult rat telencephalon. Eur J Neurosci 14:629–644.

Namba T, Mochizuki H, Onodera M, Mizuno Y, Namiki H, Seki T. 2005. The fate of neural progenitor cells expressing astrocytic and radial glial markers in the postnatal rat dentate gyrus. Eur J Neurosci 22:1928–1941.

Nelson WJ, Nusse R. 2004. Convergence of Wnt, beta-catenin, and cadherin pathways. Science 303:1483–1487.

Noctor SC, Martinez-Cerdeno V, Ivic L, Kriegstein AR. 2004. Cortical neurons arise in symmetric and asymmetric division zones and migrate through specific phases. Nat Neurosci 7:136–144.

Okano HJ, Darnell RB. 1997. A hierarchy of Hu RNA binding proteins in developing and adult neurons. J Neurosci 17:3024–3037.

Ono K, Tomasiewicz H, Magnuson T, Rutishauser U. 1994. NCAM mutation inhibits tangential neuronal migration and is phenocopied by enzymatic removal of polysialic acid. Neuron 13:595–609.

Palmer TD, Willhoite AR, Gage FH. 2000. Vascular niche for adult hippocampal neurogenesis. J Comp Neurol 425:479–494.

Parent JM. 2003. Injury-induced neurogenesis in the adult mammalian brain. Neuroscientist 9:261–272.

Petridis AK, El-Maarouf A, Rutishauser U. 2004. Polysialic acid regulates cell contact-dependent neuronal differentiation of progenitor cells from the subventricular zone. Dev Dyn 230:675–684.

Pleasure SJ, Collins AE, Lowenstein DH. 2000. Unique expression patterns of cell fate molecules delineate sequential stages of dentate gyrus development. J Neurosci 20:6095–6105.

Rakic P. 1971. Guidance of neurons migrating to the fetal monkey neocortex. Brain Res 33:471–476.

Rakic P. 2003. Developmental and evolutionary adaptations of cortical radial glia. Cereb Cortex 13:541–549.

Ribak CE, Korn MJ, Shan Z, Obenaus A. 2004. Dendritic growth cones and

recurrent basal dendrites are typical features of newly generated dentate granule cells in the adult hippocampus. Brain Res 1000:195–199.

Rutishauser U, Landmesser L. 1996. Polysialic acid in the vertebrate nervous system: a promoter of plasticity in cell-cell interactions. Trends Neurosci 19:422–427.

Sakaguchi T, Okada M, Kuno M, Kawasaki K. 1997. Dual mode of N-methyl-D-aspartate-induced neuronal death in hippocampal slice cultures in relation to N-methyl-D-aspartate receptor properties. Neuroscience 76:411–423.

Sato C, Kitajima K, Inoue S, Seki T, Troy II A, Inoue Y. 1995. Characterization of the antigenic specificity of four different anti-(2-8-linked polysialic acid) antibodies using lipid-conjugated oligo/polysialic acids. J Biol Chem 270:18923–18928.

Schmidt-Kastner R, Szymas J. 1990. Immunohistochemistry of glial fibrillary acidic protein, vimentin and S-100 protein for study of astrocytes in hippocampus of rat. J Chem Neuroanat 3:179–192.

Seki T. 2002a. Expression patterns of immature neuronal markers PSA-NCAM, CRMP-4 and NeuroD in the hippocampus of young adult and aged rodents. J Neurosci Res 70:327–334.

Seki T. 2002b. Hippocampal adult neurogenesis occurs in a microenvironment provided by PSA-NCAM-expressing immature neurons. J Neurosci Res 69:772–783.

Seki T. 2003. Microenvironmental elements supporting adult hippocampal neurogenesis. Anat Sci Int 78:69–78.

Seki T, Arai Y. 1991a. Expression of highly polysialylated NCAM in the neocortex and piriform cortex of the developing and the adult rat. Anat Embryol 184:395–401.

Seki T, Arai Y. 1991b. The persistent expression of a highly polysialylated NCAM in the dentate gyrus of the adult rat. Neurosci Res 12:503–513.

Seki T, Arai Y. 1993. Highly polysialylated neural cell adhesion molecule (NCAM-H) is expressed by newly generated granule cells in the dentate gyrus of the adult rat. J Neurosci 13:2351–2358.

Seki T, Arai Y. 1995. Age-related production of new granule cells in the adult dentate gyrus. Neuroreport 6:2479–2482.

Seki T, Rutishauser U. 1998. Removal of polysialic acid-neural cell adhesion molecule induces aberrant mossy fiber innervation and ectopic synaptogenesis in the hippocampus. J Neurosci 18:3757–3766.

Seress L, Mrzljak L. 1987. Basal dendrites of granule cells are normal features of the fetal and adult dentate gyrus of both monkey and human hippocampal formations. Brain Res 405:169–174.

Seri B, Garcia-Verdugo JM, McEwen BS, Alvarez-Buylla A. 2001. Astrocytes give rise to new neurons in the adult mammalian hippocampus. J Neurosci 21:7153–7160.

Seri B, Garcia-Verdugo JM, Collado-Morente L, McEwen BS, Alvarez-Buylla A. 2004. Cell types, lineage, and architecture of the germinal zone in the adult dentate gyrus. J Comp Neurol 478:359–378.

Shan W, Yoshida M, Wu XR, Huntley GW, Colman DR. 2002. Neural (N-) cadherin, a synaptic adhesion molecule, is induced in hippocampal mossy fiber axonal sprouts by seizure. J Neurosci Res 69:292–304.

Shapiro LA, Ribak CE. 2005. Integration of newly born dentate granule cells into adult brains: hypotheses based on normal and epileptic rodents. Brain Res Brain Res Rev 48:43–56.

Shapiro LA, Korn MJ, Shan Z, Ribak CE. 2005. GFAP-expressing radial glia-like cell bodies are involved in a one-to-one relationship with doublecortin-immunolabeled newborn neurons in the adult dentate gyrus. Brain Res 1040:81–91.

Shen Q, Goderie SK, Jin L, Karanth N, Sun Y, Abramova N, Vincent P, Pumiglia K, Temple S. 2004. Endothelial cells stimulate self-renewal and expand neurogenesis of neural stem cells. Science 304:1338–1340.

Shihabuddin LS, Horner PJ, Ray J, Gage FH. 2000. Adult spinal cord stem cells generate neurons after transplantation in the adult dentate gyrus. J Neurosci 20:8727–8735.

Shimogori T, VanSant J, Paik E, Grove EA. 2004. Members of the Wnt, Fz, and Frp gene families expressed in postnatal mouse cerebral cortex. J Comp Neurol 473:496–510.

Song H, Stevens CF, Gage FH. 2002. Astroglia induce neurogenesis from adult neural stem cells. Nature 417:39–44.

Spigelman I, Yan XX, Obenaus A, Lee EY, Wasterlain CG, Ribak CE. 1998. Dentate granule cells form novel basal dendrites in a rat model of temporal lobe epilepsy. Neuroscience 86:109–120.

Stoppini L, Buchs PA, Muller D. 1991. A simple method for organotypic cultures of nervous tissue. J Neurosci Methods 37:173–182.

Suhonen JO, Peterson DA, Ray J, Gage FH. 1996. Differentiation of adult hippocampus-derived progenitors into olfactory neurons in vivo. Nature 383:624–627.

Suzuki A, Obi K, Urabe T, Hayakawa H, Yamada M, Kaneko S, Onodera M, Mizuno Y, Mochizuki H. 2002. Feasibility of ex vivo gene therapy for neurological disorders using the new retroviral vector GCDNsap packaged in the vesicular stomatitis virus G protein. J Neurochem 82:953–960.

Tabata H, Nakajima K. 2003. Multipolar migration: the third mode of radial neuronal migration in the developing cerebral cortex. J Neurosci 23:9996–10001.

Takeichi M, Abe K. 2005. Synaptic contact dynamics controlled by cadherin and catenins. Trends Cell Biol 15:216–221.

Tamamaki N, Nakamura K, Furuta T, Asamoto K, Kaneko T. 2000. Neurons in Golgi-stain-like images revealed by GFP-adenovirus infection in vivo. Neurosci Res 38:231–236.

Tamamaki N, Nakamura K, Okamoto K, Kaneko T. 2001. Radial glia is a progenitor of neocortical neurons in the developing cerebral cortex. Neurosci Res 41:51–60.

Tanaka R, Yamashiro K, Mochizuki H, Cho N, Onodera M, Mizuno Y, Urabe T. 2004. Neurogenesis after transient global ischemia in the adult hippocampus visualized by improved retroviral vector. Stroke 35:1454–1459.

Tozuka Y, Fukuda S, Namba T, Seki T, Hisatsune T. 2005. GABAergic excitation promotes neuronal differentiation in adult hippocampal progenitor cells. Neuron 47:803–815.

van Praag H, Schinder AF, Christie BR, Toni N, Palmer TD, Gage FH. 2002. Functional neurogenesis in the adult hippocampus. Nature 415:1030–1034.

Zhao C, Teng EM, Summers RG Jr, Ming GL, Gage FH. 2006. Distinct morphological stages of dentate granule neuron maturation in the adult mouse hippocampus. J Neurosci 26:3–11.

Stable Transgene Expression in Mice Generated from Retrovirally Transduced Embryonic Stem Cells

Sanae Hamanaka[1], Tsukasa Nabekura[1], Makoto Otsu[2], Hisahiro Yoshida[3], Michio Nagata[1], Joichi Usui[2], Satoru Takahashi[1], Toshiro Nagasawa[1], Hiromitsu Nakauchi[2] and Masafumi Onodera[1]

[1]Major of Medical Sciences, Graduate School of Comprehensive Human Sciences, University of Tsukuba, Tsukuba, Ibaraki, Japan; [2]Laboratory of Stem Cell Therapy, Center for Experimental Medicine, Institute of Medical Science, The University of Tokyo, Minato-ku, Tokyo, Japan; [3]Research unit for immunogenetics, The RIKEN Research Center for Allergy and Immunology (RCAI), Turumi-ku, Yokohama, Kanagawa, Japan

Silencing of transduced genes hampers production of transgenic mice using retroviral vectors. We show stable expression of the enhanced green fluorescent protein (EGFP) gene in chimeric mice generated from retrovirally transduced embryonic stem cells. The vector was a murine stem cell virus-typed retroviral vector (GCDsap) in which the long terminal repeat and primer-binding site were derived from a PCC4 cell-passaged myeloproliferative sarcoma virus and the endogenous retrovirus dl587rev, respectively. To increase the viral titer, the vector was packaged with vesicular stomatitis virus G protein, which allowed concentration of the virus into pellets followed by resuspension in serum-free medium. In chimeric mice, EGFP was detected in various tissues including hematopoietic cells, neurons, cardiac muscle, and intestine. Furthermore, high expression was maintained in the progeny of these mice, suggesting successful germline transmission of active proviruses. Although the proportion of EGFP-expressing cells and the mean intensity of EGFP expression varied among tissues and mice, 100% of peripheral blood leukocytes expressed EGFP in mice carrying a single provirus copy, as well as in their progeny. Therefore, the gene transfer system described here provides a useful tool not only to generate transgenic animals but also to manipulate human embryonic stem cells.

Received 19 July 2006; accepted 27 October 2006; published online 19 December 2006. doi:10.1038/sj.mt.6300063

INTRODUCTION

Retroviral vectors are widely used and versatile gene transfer vehicles in gene therapy as well as basic sciences.[1] However, attenuation of transgene expression over time is a serious drawback for genetic manipulation of immature cells, such as hematopoietic or embryonic stem (ES) cells, with vectors such as those derived from the Moloney, murine leukemia virus (MoMLV).[2–4] Gene silencing is currently ascribed to *de novo* methylation of the long terminal repeat (LTR) and to inhibitory effects of transcriptional repressors that bind to responsive elements in the vector construct.[5,6] A vector containing an LTR derived from a PCC4 cell-passaged myeloproliferative sarcoma virus (PCMV), which is less susceptible to methylation than the original MoMLV-derived LTR,[7] has been demonstrated to maintain transgene expression in ES cells. Gene silencing occurs in ES cells deficient in DNA methylase and is observed within 2 days of transduction, despite the requirement more than 7 days to complete for LTR methylation,[8–10] suggesting that factors other than DNA methylation halt transgene expression. Among these, "factor A" is a repressor protein that inhibits transcription of the viral genome.[11] This protein binds to the repressor-binding site, an 18-bp DNA element overlapping the primer-binding site (PBS) located downstream of the 5'LTR of MoMLV, resulting in strong inhibition of transgene expression in immature cells.[12] One vector that exemplified this concept is the murine stem cell virus (MSCV)-typed vector, in which the LTR and PBS are derived from PCMV and the mouse endogenous retrovirus dl587rev, respectively.[13] However, continued expression in chimeric mice generated from transduced ES cells, and in their progeny, remains a challenge.[10]

We have established an improved gene transfer system using MSCV-typed retroviral vectors, allowing high transduction efficiency and continued expression of the transgene in immature cells, including hematopoietic stem cells.[14–17] A special feature of this system is that the vectors are packaged in vesicular stomatitis virus G protein by transduction into 293gpg,[18] allowing production of high-titer virus supernatants by concentration of the virus into pellets, followed by resuspension with a small amount of serum-free medium. To assess the ability of the vector system to maintain transgene expression throughout ontogenesis, chimeric mice were generated from ES cells transduced with the enhanced green fluorescent protein (EGFP) gene.

Correspondence: *Masafumi Onodera, Major of Medical Sciences, Graduate School of Comprehensive Human Sciences, University of Tsukuba, 1-1-1 Tennodai, Tsukuba, Ibaraki 305-8575, Japan. E-mail: monodera@md.tsukuba.ac.jp*

RESULTS

Stable expression of EGFP in transduced ES cells

Both the structure of the GCDsap vector encoding the full-length EGFP cDNA (**Figure 1a**) and a method used to produce the EGFP-expressing recombinant retroviruses packaged in the vesicular stomatitis virus G protein (VSV-G) envelope are described in the Materials and Methods section. The titer of the concentrated virus was approximately 2.0×10^7 infectious units (IU)/ml, as assessed on Jurkat cells. No replication-competent retrovirus was detected.

When ES cells were transduced with the EGFP gene by adding 100 μl of the concentrated virus supernatants into the culture, more than 90% of the cells expressed EGFP for up to 50 days after transduction (**Figure 1b**). On the other hand, a nearly identical vector, GC/EGFP, which contained the original MoMLV-derived PBS that contained the target sequence for the repressor protein factor A, was unable to maintain EGFP expression in transduced cells and expression rapidly declined within 5 days, falling to 12% at 38 days after transduction (**Supplementary Figure S1**). Expression was also maintained in clones arising from the GCD/EGFP-transduced ES cells that had been isolated by single-cell sorting with fluorescence-activated cell sorting (FACS) and propagation (**Supplementary Figure S2**). Although three independently established clones showed similar levels and intensities of EGFP expression, Southern blot analysis revealed that the number of provirus copies integrated into the genomes of the ES clones differed greatly (**Figure 1c**). High expression of EGFP was maintained even after differentiation into cells of bone and muscle (mesoderm; **Figure 2a–c**), squamous epithelium (ectoderm; **Figure 2d–f**), and adipose tissue (endoderm; **Figure 2g** and **h**) following development of

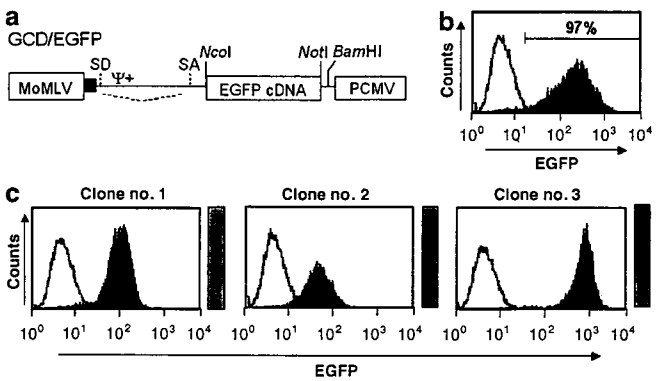

Figure 1 Structure of the retroviral vector GCD/EGFP and EGFP expression in transduced ES cells. The retroviral vector GCD/EGFP has the PCMV-derived LTR with intact splice donor (SD) and splice acceptor (SA) sequences and the EGFP cDNA is cloned between *Nco*I and *Not*I sites (**a**). The vector is cut at one site with *Bam*HI. A closed box represents the primer-binding site derived from dl587rev. Abbreviations present in the vector are labeled as follows: MoMLV, Moloney murine leukemia virus; PCMV, PCC4 cell-passaged myeloproliferative sarcoma virus; $\psi+$, packaging signal. EGFP expression in the transduced ES cells 14 days after transduction (**b**) and in three independent clones generated from progenitors sorted among ES cells (**c**) was analyzed with FACS Calibur. EGFP expression levels of untransduced ES cells are shown as solid lines. High-molecular-weight DNA was obtained from the ES clones and their provirus copy number was determined by Southern blot analysis using *Bam*HI. The number of bands hybridized with an EGFP cDNA probe is considered to be the number of provirus copies.

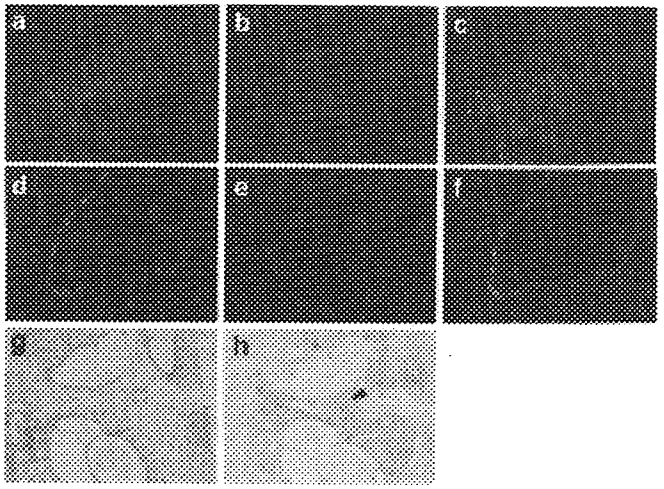

Figure 2 ES cells transduced with GCD/EGFP were transplanted intraperitoneally into sub-lethally irradiated non-obese diabetic/severe combined immunodeficient mice. Six weeks later, teratomas formed in the peritoneal cavity were excised, and sectioned with monoclonal antibodies against myoglobin (**b**) and cytokeratin (**e**) (**c** and **f** are merged images combining **a** with **b**, and **d** with **e**, respectively). Sections were stained with hematoxylin and eosin (**g**) and a monoclonal antibody against GFP (**h**). Adipose tissue areas expressing EGFP are indicated with an arrowhead.

teratomas from the transduced ES cells transplanted into non-obese diabetic/severe combined immunodeficient mice.

EGFP expression in mice derived from transduced ES cells

To assess whether the vector was capable of maintaining the expression of EGFP throughout ontogenesis, non-sorted transduced ES cells were microinjected into 3.5-day blastocysts of C57BL/6 (B6) mice within 5 days after transduction to generate chimeric mice. The birth ratio of chimeric mice, determined by coat color, was 67% (24 out of 36 mice; **Table 1**). Among those 24 mice, 17 (71%) expressed EGFP in hematopoietic lineage cells of their peripheral blood (**Figure 3a**), bone marrow (**Figure 3b**), thymus (**Figure 3c**), and spleen (**Figure 3d**). EGFP expression was also detected in other tissues, including cerebrum (**Figure 3e**), cerebellum (**Figure 3f**), cardiac muscle (**Figure 3g**), and intestinal tracts (**Figure 3h**). The expression was also maintained through F1 mice into F2 mice generated by mating B6 mice (**Figures 3i, j,** and **4** and **Table 1**). Southern blot analysis revealed that each genome-integrated provirus copy was independently transmitted to gametes, resulting in the generation of F1 and F2 mice with different integration patterns by fertilization with gametes of B6 mice. Interestingly, a chimeric mouse shown in **Figure 4** gave birth to F1 mice that could be categorized into three groups based on the level of EGFP expression (high, intermediate, and low), and all F1 mice in each group showed an identical provirus integration pattern. Furthermore, only mice with high EGFP expression (**Figure 4**, left panels) gave birth to F2 mice that also highly expressed EGFP. The integration pattern in the F2 mice was identical to that in their parents, suggesting that the proviruses integrated in

these mice were not silenced through multiple rounds of gametogenesis and development.

Correlation between provirus copy number and EGFP expression level

To assess correlation between provirus copy number and EGFP expression level, high-molecular-weight DNA was obtained from mice with various percentages of EGFP-expressing cells in the peripheral blood, and provirus copy numbers were determined by Southern blot analysis (**Figure 5**). Four chimeric mice (lanes 1–4) showed different integrated patterns. Their progeny (lanes 5–9 from mouse 1 and lanes 10–13 from mouse 4) inherited provirus copies from their parents independently. The number of provirus copies integrated into the genomes of F1 mice varied substantially from mouse to mouse, ranging from 2 to 7. Interestingly, mice with a large number of provirus copies did not always strongly express EGFP strong (lanes 6 and 10), whereas EGFP expression was observed in mice with fewer provirus copies (lanes 5 and 13). F2 mice born from mouse 13 seemed to be divided into two groups: those with weak EGFP expression (lane 14) and those with strong expression (lanes 15–17). Finally, 100% of peripheral blood leukocytes of F3 mice with a single provirus copy, indicated by the arrowhead (lanes 18 and 19), expressed EGFP. This was also true for F5 mice (lanes 22 and 23). Detailed analysis of the integration site is under way using linker amplification-mediated PCR.[25] No tumorigenesis has been observed in chimeric mice and their progeny over 1 year.

Table 1 Birth ratios and EGFP expression[a] in transgenic mice

	Mice with transduced ES-derived cells	Mice with EGFP-expressing hematopoietic cells
Chimeric mice	24/36 (67%)	17/24 (71%)
F1 mice[b]	95/114 (83%)	47/95 (49%)
F2 mice[c]		32/56 (57%)

EGFP, enhanced green fluorescence protein; ES, embryonic stem. [a]Results present the number of indicated mice/total mice (percentage of indicated mice). [b]F1 mice were born from four chimeric mice with EGFP expression. [c]F2 mice were born from two F1 mice with EGFP expression.

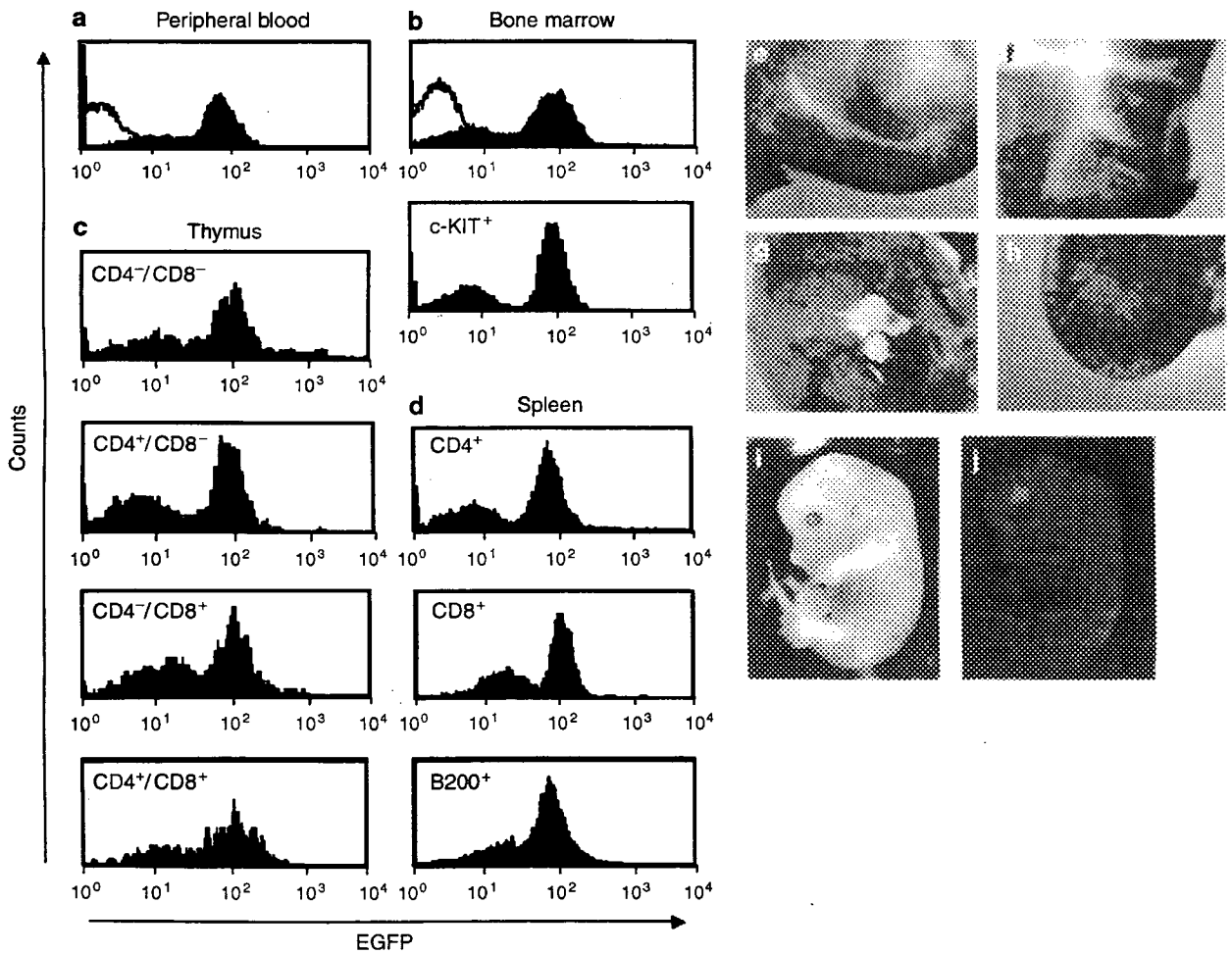

Figure 3 EGFP expression in chimeric mice. EGFP expression was detected in hematopoietic cells of peripheral blood (**a**), total bone marrow population (**b**), thymus (**c**), and spleen (**d**). Results of histograms in which cell populations are indicated present EGFP expression patterns of the cell population gated by FACS Calibur. A solid line represents EGFP expression levels of untransduced ES cells. EGFP expression was also detected in various tissues including cortical areas of the cerebrum (**e**), the granular layer to molecular layer of the cerebellum (**f**), cardiac muscle and Purkinje fibers of the hearts (**g**), and villi and Auerbach's and Meissner's neuroplexus of intestinal tracts (**h**). An F1 mouse embryo at 13.5 days post coitum with stereomicroscopy (**i**) and fluorescence microscopy (**j**).

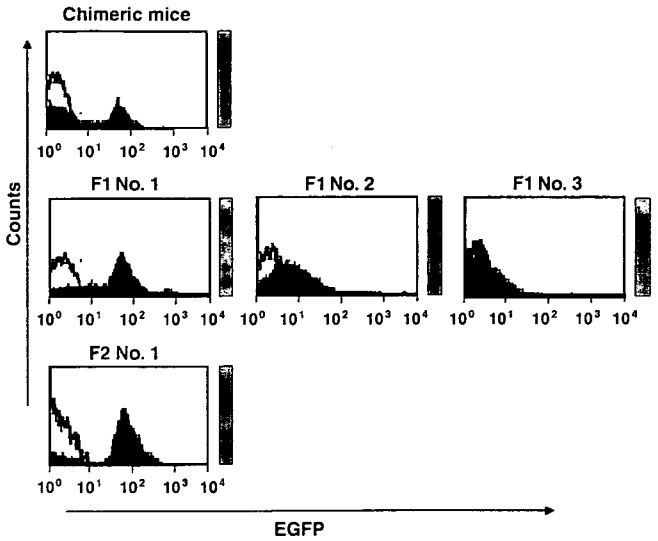

Figure 4 EGFP expression and integration patterns from a chimeric mouse to F2 mice. A chimeric mouse gave birth to F1 mice that could be categorized into three groups by the level of EGFP expression (high F1 No. 1, intermediate F1 No. 2, and low F1 No. 3). F1 No. 1 gave birth to F2 mice with high EGFP expression (F2 No. 1). An integration pattern of provirus copies in each mouse, as determined by Southern blot analysis, is presented together with FACS analysis. A solid line represents EGFP expression levels of untransduced ES cells.

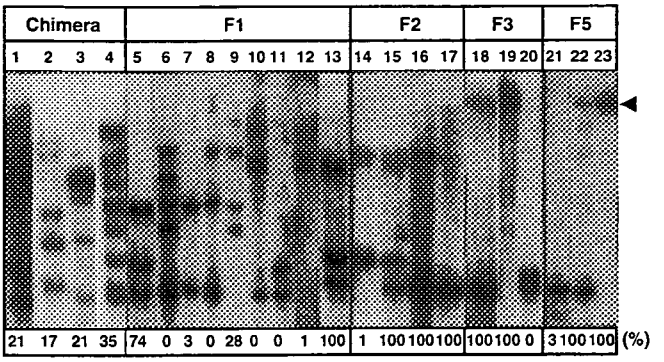

Figure 5 Correlation between provirus copy number and EGFP expression level. High-molecular-weight DNA was obtained from mice with various percentages of EGFP-expressing cells and their provirus copy numbers were determined by Southern blot analysis. Four chimeric mice with similar EGFP expression levels were analyzed (lanes 1–4). F1 mice (lanes 5–9 and lanes 10–13) were born from the chimeric mice whose samples are in lanes 1 and 4, respectively. All F2 mice were born to mouse 13 and all F3 mice were born to mouse 17. The percentages of EGFP-expressing cells in the peripheral blood are indicated below.

DISCUSSION

This study has demonstrated that the retroviral vector GCDsap packaged in the VSV-G envelope allowed stable transgene expression in mice generated from ES cells transduced with the EGFP gene. This is the first report, to our knowledge, that vectors derived from an oncoretrovirus are capable of maintaining transgene expression in transgenic mice throughout ontogenesis. Successful germline transmission of active provirus copies, resulting in maintenance of expression in their progeny, should be especially noted. The high success rate of generation of transgenic mice observed in the present study may be mainly attributed to the specific vector construct and viral envelope used, as an identical vector to GCDsap except for the PBS, GCsap,[26] which has the original MoMLV-derived PBS while carrying the PCMV-derived LTR, was not capable of maintaining EGFP expression in ES cells (data not shown). Of importance is that GCsap and GCDsap differed only in whether or not they harbored the target sequences for the negative transcription factor, factor A.[27] As the MoMLV-derived PBS functioned as a strong repressor for any promoter,[12] the binding of factor A to the PBS may exercise a decisive influence on silencing of transgene expression in ES cells.

Given the critical involvement of the PBS in gene silencing in ES cells, however, another important question is why conventional MSCV-typed retroviral vectors have not achieved continued transgene expression in chimeric mice.[10] This also is partly owing to the vector construct, in that the GCDsap is a spliced-type vector like the MFG vector that provides higher levels of transgene expression per provirus.[19,26] However, the main reason is likely that high-titer virus supernatants could be prepared by packaging the vector within the VSV-G envelope, resulting in high transduction efficiency of ES cells. This has both in mice and in other species.[30–32] Considering that the provirus copy number in ES cells transduced with conventional retroviral vectors was not higher than that obtained with lentiviral vectors,[28,29,33] the high transduction efficiency obtained from the present study should be noted. It is often suggested that the higher the provirus copy number, the greater the transgene expression.[34] Our results, in which mice with a single provirus copy expressed EGFP strongly, might suggest that high transduction efficiency increases the probability of integration into sites relevant for maintenance of transgene expression. If so, a detailed analysis of integration sites may permit identification of sites that are buffered from inactivation throughout morphogenesis.

As the yield of transgenic mice in the present study was comparable to that obtained with conventional methods, retroviral infection *per se* likely had no deleterious effects on the ability of ES cells to generate chimeric mice. With the vector system, ES cells can be multi-infected with retroviruses that incorporate different markers, allowing analysis of interactions of multiple genes. Furthermore, the system may lead to wider selection of mice that express the transgene in appropriate tissues or at required levels based on different integration sites. This method is technically less demanding and allows infection of various species by using the VSV-G envelope.[35] It might be useful for genetic modification of ES cells derived from any species, including human beings. Thus, the gene transfer method described here assists in the production of transgenic animals. It may also provide useful tools to develop future combination therapies of genetic and regenerative medicine using human ES cells.

MATERIALS AND METHODS

Mice. C57BL/6 mice were purchased from Nihon Clea (Tokyo, Japan) and Charles River Japan (Yokohama, Japan). All experiments were performed under institutional guidelines.

Retroviral vectors. GCsap(MoMLV)[19] was digested with *Hin*dIII and *Sac*I to replace fragments containing the MoMLV-derived 3′LTR with corresponding *Hin*dIII–*Sac*I fragments of the PCMV-derived 3′LTR from pMSCV-neoEB[14] (GCsap(PCMV)). The vector was further digested with *Sac*I and *Eco*RI to replace fragments containing 5′LTR and the PBS derived from MoMLV with the corresponding 5′LTR and PBS of the MND vector. The PBS of the MND vector is derived from dl587rev[20] (GCDsap(PCMV)). *Nco*I–*Not*I fragments of EGFP cDNA were inserted into the *Nco*I–*Not*I-digested vector to generate GCD/EGFP. The vector was converted to corresponding retroviruses packaged in VSV-G envelope by transduction into 293gp.[21] The viral titer of GCD/EGFP was approximately 2.0×10^7 IU/ml as assessed on Jurkat cells.

Transduction into ES cells. Mouse ES cells (E14) were cultured according to supplier's recommendations.[22] Single-cell suspensions were transduced once by adding 100 μl of the concentrated virus supernatants to the culture at a multiplicity of infection of 1. The number of EGFP-positive cells and the mean florescent protein intensity were quantified by FACS Calibur or FACS Vantage (Becton Dickinson, San Jose, CA). Teratomas were obtained from sub-lethally irradiated (250 cGy) non-obese diabetic/severe combined immunodeficient mice (Sankyo Lab Service, Tokyo, Japan) that had been transplanted intraperitoneally qwith single-cell suspensions of 5×10^6 transduced ES cells. Six weeks after transplantation, resultant tumors were harvested, fixed in 4% paraformaldehyde before freezing in OCT medium (Tissue Tek, Sakura Finetek, Torrance, CA), and cryostat-sectioned. Parallel sections were stained with anti-myoglobin (Dako, Kyoto, Japan) or anti-cytokeratin (Zymed, San Francisco, CA) antibodies that were detected with Cy3-conjugated anti-rabbit IgG antibody (Amersham Biosciences Corp., Piscataway, NJ). Three-micrometer sections were also stained with hematoxylin and eosin, and counterstained with rabbit anti-GFP antibody (Molecular Probes, Eugene, OR) that was detected with diaminobenzidine (DAB, Dojin Chem, Kumamoto, Japan).

Generation of chimeric mice. Chimeric mice were generated by a conventional method where the EGFP-transduced ES cells were microinjected into day 3.5 blastocysts of B6 mice, followed by transferring to host uteri.[23] The resultant chimeric mice were mated with B6 mice to obtain their progeny. Whole-mount immunohistostaining was performed by a method described elsewhere.[24] Samples were examined using Axioplan 2 and AxioVision 3.1 softwares (Carl Zeiss, Oberkochen, Germany).

Cell surface analysis. Hematopoietic cells were stained with phycoerythrin-conjugated rat anti-mouse CD4 (RM4-5), CD8 (53-6.7), Mac-1 (M1/70), Ter119 (Ter119), and NK1.1 (PK136) antibodies; allophycocyanin-conjugated rat anti-mouse B220 (RA3-6B2), Gr-1 (RB6-8C5), and c-KIT (2B8) antibodies; and phycoerythrin-Cy5-conjugated rat anti-mouse CD3 (142-2C11), CD4 (RM4-5), and B220 (RA-6B2) antibodies. After being washed with phosphate-buffered saline containing 2% fetal calf serum, stained cells were analyzed by FACS Calibur or FACS Vantage. All reagents were purchased from BD Biosciences PharMingen (San Diego, CA).

Southern blot analysis. High-molecular-weight DNA was obtained from transduced ES cells or mouse tails. Twenty micrograms of genomic DNA was digested with *Bam*HI, electrophoresed in 1% agarose gel, transferred to a nylon membrane, and hybridized to [α-^{32}P]dCTP (deoxycytidine 5′-triphosphate) labeled EGFP cDNA. The restriction enzyme *Bam*HI cuts the vector at one site and therefore the number of fragments hybridized with the probe is considered to be the number of provirus copies integrated in host genomes.

ACKNOWLEDGMENTS

We thank Alex Knisely (King's College Hospital) and Rudolf Jaenisch (Massachusetts Institute of Technology) for providing a critical review of the manuscript, and Ms Naoko Okano for excellent secretarial assistance. This work was supported in part by grants from the Monbu-Kagaku-Sho (MO).

SUPPLEMENTARY MATERIAL

Figure S1. Comparison of two retroviral vectors analyzed.
Figure S2. ES cells transduced with GCD/EGFP were sorted by FACS and EGFP expression was analysed on the indicated day.

REFERENCES

1. Verma, IM and Weitzman, MD (2005). Gene therapy: twenty-first century medicine. *Annu Rev Biochem* **74**: 711–738.
2. Jaenisch, R (1976). Germ line integration and Mendelian transmission of the exogenous Moloney leukemia virus. *Proc Natl Acad Sci USA* **73**: 1260–1264.
3. Robertson, E, Bradley, A, Kuehn, M and Evans, M (1986). Germ-line transmission of genes introduced into cultured pluripotential cells by retroviral vector. *Nature* **323**: 445–448.
4. Jahner, D *et al.* (1982). *De novo* methylation and expression of retroviral genomes during mouse embryogenesis. *Nature* **298**: 623–628.
5. Flanagan, JR, Krieg, AM, Max, EE and Khan, AS (1989). Negative control region at the 5′ end of murine leukemia virus long terminal repeats. *Mol Cell Biol* **9**: 739–746.
6. Swindle, CS, Kim, HG and Klug, CA (2004). Mutation of CpGs in the murine stem cell virus retroviral vector long terminal repeat represses silencing in embryonic stem cells. *J Biol Chem* **279**: 34–41.
7. Franz, T, Hilberg, F, Seliger, B, Stocking, C and Ostertag, W (1986). Retroviral mutants efficiently expressed in embryonal carcinoma cells. *Proc Natl Acad Sci USA* **83**: 3292–3296.
8. Grez, M, Akgun, E, Hilberg, F and Ostertag, W (1990). Embryonic stem cell virus, a recombinant murine retrovirus with expression in embryonic stem cells. *Proc Natl Acad Sci USA* **87**: 9202–9206.
9. Pannell, D *et al* (2000). Retrovirus vector silencing is *de novo* methylase independent and marked by a repressive histone code. *EMBO J* **19**: 5884–5894.
10. Cherry, SR, Biniszkiewicz, D, Van, PL, Baltimore, D and Jaenisch, R (2000). Retroviral expression in embryonic stem cells and hematopoietic stem cells. *Mol Cell Biol* **20**: 7419–7426.
11. Laker, C *et al.* (1998). Host *cis*-mediated extinction of a retrovirus permissive for expression in embryonal stem cells during differentiation. *J Virol* **72**: 339–348.
12. Loh, TP, Sievert, LL and Scott, RW (1990). Evidence for a stem cell-specific repressor of Moloney murine leukemia virus expression in embryonal carcinoma cells. *Mol Cell Biol* **10**: 4045–4057.
13. Haas, DL *et al.* (2003). The Moloney murine leukemia virus repressor binding site represses expression in murine and human hematopoietic stem cells. *J Virol* **77**: 9439–9450.
14. Hawley, RG, Lieu, FH, Fong, AZ and Hawley, TS (1994). Versatile retroviral vectors for potential use in gene therapy. *Gene Ther* **1**: 136–138.
15. Nabekura, T, Otsu, M, Nagasawa, T, Nakauchi, H and Onodera, M (2006). Potent vaccine therapy with dendritic cells genetically modified by the gene-silencing-resistant retroviral vector GCDNsap. *Mol Ther* **13**: 301–309.
16. Yamada, M, Onodera, M, Mizuno, Y and Mochizuki, H (2004). Neurogenesis in olfactory bulb identified by retroviral labeling in normal and 1-methyl-4-phenyl-1,2,3,6-tetrahydropyridine-treated adult mice. *Neuroscience* **124**: 173–181.
17. Suzuki, A *et al.* (2002). Clonal identification and characterization of self-renewing pluripotent stem cells in the developing liver. *J Cell Biol* **56**: 173–184.
18. Ory, DS, Neugeboren, BA and Mulligan, RC (1996). A stable human-derived packaging cell line for production of high titer retrovirus/vesicular stomatitis virus G pseudotypes. *Proc Natl Acad Sci USA* **93**: 11400–11406.
19. Onodera, M *et al.* (1998). Development of improved adenosine deaminase retroviral vectors. *J Virol* **72**: 1769–1774.
20. Halene, S, Wang, L, Cooper, RM, Bockstoce, DC, Robbins, PB and Kohn, DB (1999). Improved expression in hematopoietic and lymphoid cells in mice after transplantation of bone marrow transduced with a modified retroviral vector. *Blood* **94**: 3349–3357.
21. Suzuki, A *et al.* (2002). Feasibility of *ex vivo* gene therapy for neurological disorders using the new retroviral vector GCDNsap packaged in the vesicular stomatitis virus G protein. *J Neurochem* **82**: 953–960.
22. Doetschman, TC, Eistetter, H, Katz, M, Schmidt, W and Kemler, R (1985). The *in vitro* development of blastocyst-derived embryonic stem cell lines: formation of visceral yolk sac, blood islands and myocardium. *J Embryol Exp Morphol* **87**: 27–45.
23. Joyner, AL (1993). *Gene Targeting: A Practical Approach.* Oxford University Press: Oxford.
24. Yoshida, H, Kunisada, T, Kusakabe, M, Nishikawa, S and Nishikawa, S-I (1996). Distinct stages of melanocyte differentiation revealed by analysis of nonuniform pigmentation patterns. *Development* **122**: 1207–1214.
25. Schmidt, M *et al.* (2002). Polyclonal long-term repopulating stem cell clones in a primate model. *Blood* **100**: 2737–2743.
26. Kaneko, S, Onodera, M, Fujiki, Y, Nagasawa, T and Nakauchi, H (2001). Simplified retroviral vector gcsap with murine stem cell virus long terminal repeat allows high and continued expression of enhanced green fluorescent protein by human

hematopoietic progenitors engrafted in nonobese diabetic/severe combined immunodeficient mice. *Hum Gene Ther* **12**: 35–44.

27. Yamauchi, M, Freitag, B, Khan, C, Berwin, B and Barklis, E (1995). Stem cell factor binding to retrovirus primer binding site silencers. *J Virol* **69**: 1142–1149.
28. Pfeifer, A, Ikawa, M, Dayn, Y and Verma, IM (2002). Transgenesis by lentiviral vectors: lack of gene silencing in mammalian embryonic stem cells and preimplantation embryos. *Proc Natl Acad Sci USA* **99**: 2140–2145.
29. Lois, C, Hong, EJ, Pease, S, Brown, EJ and Baltimore, D (2002). Germline transmission and tissue-specific expression of transgenes delivered by lentiviral vectors. *Science* **295**: 868–872.
30. Gaiano, N, Allende, M, Amsterdam, A, Kawakami, K and Hopkins, N (1996). Highly efficient germ-line transmission of proviral insertions in zebrafish. *Proc Natl Acad Sci USA* **93**: 7777–7782.
31. Chan, AWSE, Homan, J, Ballou, LU, Burns, JC and Bremel, RD (1998). Transgenic cattle produced by reverse-transcribed gene transfer in oocytes. *Proc Natl Acad Sci USA* **95**: 14028–14033.
32. Chan, AWS, Chong, KY, Martinovich, C, Simerly, C and Schatten, G (2001). Transgenic monkeys produced by retroviral gene transfer into mature oocytes. *Science* **291**: 309–312.
33. Hamaguchi, I *et al.* (2000). Lentivirus vector gene expression during ES cell-derived hematopoietic development *in vitro*. *J Virol* **74**: 10778–10784.
34. Kustikova, OS *et al.* (2003). Dose finding with retroviral vectors: correlation of retroviral vector copy numbers in single cells with gene transfer efficiency in a cell population. *Blood* **102**: 3934–3937.
35. Emi, N, Friedmann, T and Yee, JK (1991). Pseudotype formation of murine leukemia virus with the G protein of vesicular stomatitis virus. *J Virol* **65**: 1202–1207.

Gene and cell therapy for relapsed leukemia after allo-stem cell transplantation

Masafumi Onodera
Advanced Biomedical Applications, Graduate School of Comprehensive Human Sciences, University of Tsukuba, Japan

Abstract

Donor lymphocytes function as a double-edged sword in allogeneic stem cell transplantation (allo-SCT), that is, they attack leukemic cells (graft versus leukemia, GVL) as well as patient's normal tissues such as liver, intestines, and skin (graft versus host disease, GVHD). The strong GVL reaction has made infusions of donor lymphocytes (DLI) an effective treatment for relapsed leukemia after allo-SCT, especially for relapse of chronic myelogenous leukemia. However, the use of DLI is severely limited by the risk of a potential life-threatening complication, GVHD.

In 2004, we started a phase I/II clinical trial of DLI using donor lymphocytes transduced with the retroviral vector SFCMM-3 that expressed the herpes simplex virus thymidine kinase gene for patients with relapsed leukemia after allo-SCT at the Tsukuba University Hospital. The TK-DLI is aimed at control of severe GVHD by administration of ganciclovir (GCV) if it occurs while maintaining the maximum GVL effects. So far, we have done nine transduction procedures and infused the donor lymphocytes into five patients (2 AML, 2 ALL, and 1 MDS). All patients received approximately $1x10^6$ cells per kilogram of body weight. In the result, four out of five patients showed some clinical responses such as inhibition of leukemic cell growth, mitigation of lymph node swelling, and lowing the values of molecular markers of tumors after infusions of the transduced cells. One AML patient achieved complete remission and no relapse signs have been observed over 1 year after the treatment. Two patients developed GVHD (1 acute and 1 chronic) and the acute GVHD (grade III) was successfully controlled by administration of GVC, in the absence of immunosuppressive drugs. No adverse effects related to gene therapy have been observed. The clinical trials confirmed the therapeutic potential and safety of TK-DLI as a treatment for relapsed leukemia and the effectiveness of in vivo administration of GCV to eradicate the transduced cells. The TK-DLI is expected to offer the potential of a safer and more effective adoptive immune cell therapy for patients with hematologic malignancies in combination with allo-SCT.
(Gene Therapy 2007; p286-294, 2007)

Keywords: gene therapy, retroviral vector, suicide gene, graft-versus-leukemia, donor lymphocyte infusion

Masafumi Onodera
Contact address: Advanced Biomedical Applications, Graduate School of Comprehensive Human Sciences, University of Tsukuba, 1-1-1 Tennodai, Tsukuba, 305-8575, Japan
E-mail: monodera@md.tsukuba.ac.jp

Introduction

Transplantation of hematopoietic stem cells (HSCs) from HLA-matched related donors following both high-dose systemic chemotherapy and total-body irradiation (TBI) is the most effective treatment for patients with hematological malignancies (1-3). The